On the convergence of the harmonic B_z algorithm in magnetic resonance electrical impedance tomography

Jijun Liu, Jin Keun Seo, Mourad Sini, Eung. Je Woo

On the convergence of the harmonic B_z algorithm in magnetic resonance electrical impedance tomography

J.J. Liu* J.K. Seo† M. Sini ‡ E.J. Woo §

March 3, 2007

Abstract. Magnetic Resonance Electrical Impedance Tomography (MREIT) is a new medical imaging technique that aims to provide electrical conductivity images with sufficiently high spatial resolution and accuracy. A new MREIT image reconstruction method called the harmonic B_z algorithm was proposed in 2002 and it is based on the measurement of B_z that is a single component of an induced magnetic flux density $\mathbf{B} = (B_x, B_y, B_z)$ subject to an injection current. Since then, MREIT imaging techniques have made significant progress and recent published numerical simulations and phantom experiments show that we can produce high-quality conductivity images when the conductivity contrast is not very high. Though numerical simulations can explain why we could successfully distinguish different tissues with small conductivity differences, a rigorous mathematical analysis is required to better understand the underlying physical and mathematical principle. The purpose of this paper is to provide such a mathematical analysis of these numerical simulation and experimental results. By using a uniform *a priori* estimate for the solution of the elliptic equation in the divergent form and an induction argument, we show that, for a relatively small contrast of the target conductivity, the iterative harmonic B_z algorithm with a good initial guess is stable and exponentially convergent in the continuous norm. Both two and three-dimensional versions of the algorithm are considered and the difference in the convergence property of these two cases is analyzed. Some numerical results are also given to show the expected exponential convergence behavior.

Keywords: MREIT, conductivity, image reconstruction, convergence

AMS Classifications: 35R30,35J05,76Q05

1 Introduction

Magnetic Resonance Electrical Impedance Tomography (MREIT) is an electrical conductivity imaging technique using an MRI scanner with a current injection apparatus. Since the early 1980s, there have been significant efforts to produce cross-sectional images of a

*Department of Mathematics, Southeast University, Nanjing, 210096, email: jjliu@seu.edu.cn, P.R.China.

†Department of Mathematics, Yonsei University, Seoul, 120-749, email: seoj@yonsei.ac.kr, Korea.

‡Department of Mathematics, Yonsei University, Seoul, 120-749, email: sini@yonsei.ac.kr, Korea.

§College of Electronics and Information, Kyung Hee University, Kyungki, 449-701, email: ejwoo@khu.ac.kr, Korea.

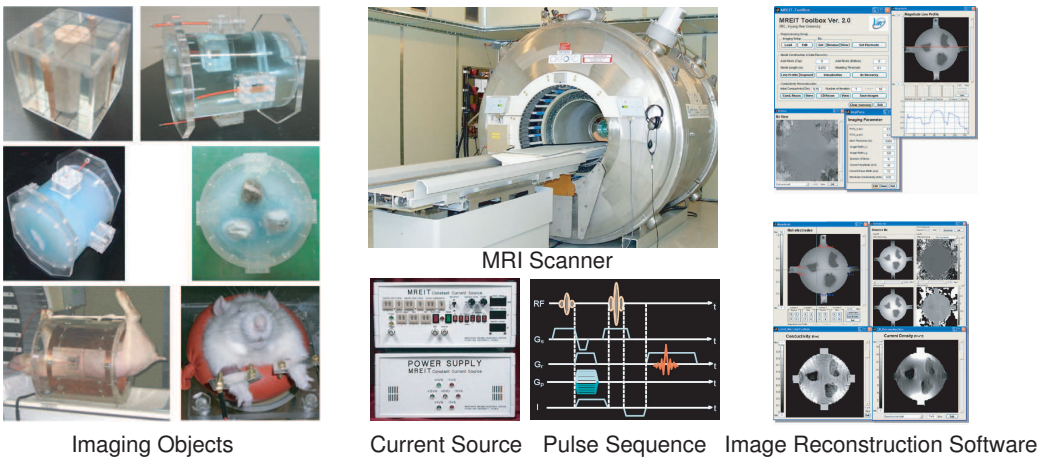

Figure 1: MREIT system at Impedance Imaging Research Center in Korea and image reconstruction software.

conductivity distribution σ inside a three-dimensional body Ω using boundary measurements of current-voltage data (Neumann-to-Dirichelt data) entering the elliptic equation $\nabla \cdot (\sigma \nabla u) = 0$ in Ω, and this technique has been called Electrical Impedance Tomography (EIT) [6, 16, 25]. Here, u denotes the electric potential inside Ω. However, EIT has suffered from the well-known ill-posedness of the corresponding inverse problem related with the insensitivity of Cauchy data on the boundary $\partial\Omega$ to any internal local change of σ. Acquisition of more accurate Cauchy data on $\partial\Omega$ requires a sophisticated EIT instrument and a large number of surface electrodes. However, in practice, the cumbersome procedure to attach many electrodes are prone to increase measurement errors in addition to electronic noise and various artifacts. Furthermore, there exist uncertainties in terms of electrode positions and boundary shape of an imaging subject. Due to the ill-posedness and the errors originating from these practical difficulties, the spatial resolution and accuracy of EIT images are relatively poor and therefore its practical applicability has been quite limited.

On the other hand, MREIT takes advantage of the internal information of B_z, the z-component of the magnetic flux density distribution $\mathbf{B} = (B_x, B_y, B_z)$ induced by the internal current density $\mathbf{J} = -\sigma \nabla u$ subject to an injection current through a pair of surface electrodes. The B_z data can be measured by using an MRI scanner as illustrated in Figure 1. Here z-axis is the direction of the main magnetic field of the MRI scanner. MREIT utilizes the fact that the data B_z convey the information about any local change of σ via the Biot-Savart law:

$$B_z(x,y,z) = \frac{\mu_0}{4\pi} \int_\Omega \frac{\sigma(\mathbf{r}) \left[(x-x') \frac{\partial u}{\partial y}(\mathbf{r}') - (y-y') \frac{\partial u}{\partial x}(\mathbf{r}') \right]}{|\mathbf{r} - \mathbf{r}'|^3} \, d\mathbf{r}', \ \mathbf{r} = (x,y,z) \in \Omega.$$

This supplementary use of the internal B_z data enables MREIT to bypass the ill-posedness problem in EIT. In early 2002, the first constructive B_z-based MREIT algorithm called the harmonic B_z algorithm was proposed in [20]. Since then, MREIT has been advanced rapidly and now is at the stage of animal experiments ([15]).

The harmonic B_z algorithm is based on the following curl of the Ampere law:

$$\frac{1}{\mu_0} \Delta B_z = \langle \nabla \sigma \, , \, \begin{pmatrix} 0 & 1 & 0 \\ -1 & 0 & 0 \\ 0 & 0 & 0 \end{pmatrix} \nabla u \rangle, \tag{1.1}$$

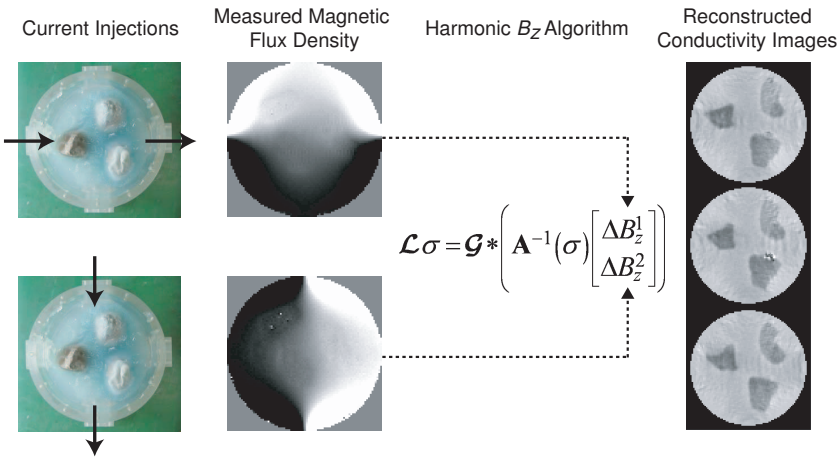

Figure 2: Overview of the harmonic B_z algorithm.

where μ_0 is the magnetic permeability of the free space, $\langle \cdot, \cdot \rangle$ inner product, and Δ denotes the Laplacian. Recent published numerical simulations and phantom experiments show that conductivity images with high spatial resolution are achievable [11, 12, 17, 18, 19, 23]. Figure 2 shows a schematic diagram of the harmonic B_z algorithm and typical MREIT images of a conductivity phantom including three chunks of biological tissues having different conductivity values inside a cylindrical container Ω.

Although the harmonic B_z algorithm shows a remarkable performance in various numerical simulations and phantom experiments, rigorous mathematical theories regarding its convergence behavior have not been supported yet. The purpose of this paper is to deal with this convergence analysis rigorously. For a suitably constructed admissible iteration set in terms of *a priori* information about the target conductivity, we can prove that the sequence $\{\sigma^n\}$ is uniformly bounded by a uniform estimate on the solution to the elliptic equation in the divergent form. Using this *a priori* estimate and an induction argument, we show that, in both two and three-dimensional cases, the harmonic B_z algorithm is stable and exponentially convergent, provided that the contrast of the target conductivity distribution is not very high. It is impossible to get the C^1 convergence in the three-dimensional problem even when the harmonic B_z algorithm is applied to a target conductivity with small contrast. This mathematical difficulty comes from the algorithm itself. With this theoretical result, we partially answer the question on the applicable scope of the harmonic B_z algorithm and explain the quickly convergent phenomena arising in numerical tests. We wish to refer to our recent article [14], which briefly discusses this convergence issue using special examples of two-dimensional conductivity distributions.

It seems that the small contrast in the target conductivity is necessary for the convergence of the harmonic B_z iteration scheme, provided that the input current is not so large. This phenomena can be explained physically. For a given input current from the boundary, if the conductivity has a large jump inside the medium, then the current going through will be small and therefore the magnetic flux density will also be weak. For a relatively high contrast of the conductivity distribution, the algorithm needs to be adapted to control the amplification of this contrast in the iteration process. This issue should be considered in the future.

2 Exact mathematical model of MREIT

Since our goal is to use MREIT techniques in practical clinical applications, we must set up an exact mathematical model of MREIT that agrees with a planed medical imaging system. To simplify our study, let us make several assumptions which should not go astray from the practical model. Let the subject to be imaged occupy a three-dimensional bounded domain $\Omega \subset \mathbb{R}^3$ with a smooth connected boundary $\partial\Omega$ and each $\Omega_{z_0} := \Omega \cap \{z = z_0\} \subset \mathbb{R}^2$, the slice of Ω cut by the plane $\{z = z_0\}$, has a smooth connected boundary. We assume that the conductivity distribution σ of the subject Ω is isotropic, $C^1(\overline{\Omega})$, and $0 < \sigma_- < \sigma < \sigma_+$ with two known constants $\sigma_\pm$. Though σ is usually piecewise-smooth in practice, this can be approximated by $C^1(\overline{\Omega})$ function and so it is a matter of how big $\|\sigma\|_{C^1(\Omega)}$ is. We attach a pair of copper electrodes $\mathcal{E}^+$ and $\mathcal{E}^-$ on $\partial\Omega$ in order to inject current, and let $\mathcal{E}^+ \cup \mathcal{E}^-$ be the portion of the surface $\partial\Omega$ where electrodes are attached, see Figure 2.

The injection current I produces an internal current density $\mathbf{J} = (J_x, J_y, J_z)$ inside the subject Ω satisfying the following problem:

$$\begin{cases} \nabla \cdot \mathbf{J} = 0 \quad \text{in } \Omega \\ I = -\int_{\mathcal{E}^+} \mathbf{J} \cdot \mathbf{n} ds = \int_{\mathcal{E}^-} \mathbf{J} \cdot \mathbf{n} ds, \quad \mathbf{J} \times \mathbf{n} = 0 \ \text{ on } \mathcal{E}^+ \cup \mathcal{E}^- \\ \mathbf{J} \cdot \mathbf{n} = 0 \quad \text{on } \partial\Omega \setminus \overline{\mathcal{E}^+ \cup \mathcal{E}^-}, \end{cases} \tag{2.1}$$

where $\mathbf{n}$ is the outward unit normal vector on $\partial\Omega$ and ds the surface area element. The condition of $\mathbf{J} \times \mathbf{n} = 0$ on $\mathcal{E}^+ \cup \mathcal{E}^-$ comes from the fact that copper electrodes are perfect conductors. Since $\mathbf{J}$ is expressed as $\mathbf{J} = -\sigma\nabla u$ where u is the corresponding electrical potential, (2.1) can be converted to

$$\begin{cases} \nabla \cdot (\sigma \nabla u) = 0 \quad \text{in } \Omega \\ I = \int_{\mathcal{E}^+} \sigma \frac{\partial u}{\partial \mathbf{n}} \, ds = -\int_{\mathcal{E}^-} \sigma \frac{\partial u}{\partial \mathbf{n}} ds, \quad \nabla u \times \mathbf{n} = 0 \ \text{ on } \mathcal{E}^+ \cup \mathcal{E}^- \\ \sigma \frac{\partial u}{\partial \mathbf{n}} = 0 \quad \text{on } \partial\Omega \setminus \overline{\mathcal{E}^+ \cup \mathcal{E}^-}, \end{cases} \tag{2.2}$$

where $\frac{\partial u}{\partial \mathbf{n}} = \nabla u \cdot \mathbf{n}$. The above nonstandard boundary value problem (2.2) is well-posed and has a unique solution up to a constant. We omit the proof of the uniqueness (up to a constant) within the class $W^{1,2}(\Omega)$ since it follows from the standard argument in PDE.

Let us briefly discuss the boundary conditions that are essentially related with the size of electrodes. The condition $\nabla u \times \mathbf{n}|_{\mathcal{E}^\pm} = 0$ ensures that each of $u|_{\mathcal{E}^+}$ and $u|_{\mathcal{E}^-}$ is a constant, since ∇u is normal to its level surface. The term $\pm I = \int_{\mathcal{E}^\pm} \sigma \frac{\partial u}{\partial \mathbf{n}} \, ds$ means that the total amount of injection current through the electrodes is I mA. Let us denote $g := -\sigma \frac{\partial u}{\partial \mathbf{n}}|_{\partial\Omega}$. In practice, it is difficult to specify the Neumann data g in a point-wise sense because only the total amount of injection current I is known. It should be noticed that the boundary condition in (2.2) leads $|g| = \infty$ on $\partial\mathcal{E}^\pm$, singularity along the boundary of electrodes, and $g \notin L^2(\partial\Omega)$. But, fortunately $g \in H^{-1/2}(\partial\Omega)$, which also can be proven by the standard regularity theory in PDE.

The exact model (2.2) can be converted into the following standard problem of elliptic equation with mixed boundary conditions.

Lemma 2.1. *Assume that $\tilde{u}$ solves*

$$\begin{cases} \nabla \cdot (\sigma \nabla \tilde{u}) = 0 \quad in \quad \Omega \\ \tilde{u}|_{\mathcal{E}^+} = 1, \ \tilde{u}|_{\mathcal{E}^-} = 0 \\ -\sigma \frac{\partial \tilde{u}}{\partial \mathbf{n}} = 0 \quad on \quad \partial\Omega \setminus (\mathcal{E}^+ \bigcup \mathcal{E}^-). \end{cases} \tag{2.3}$$

If u is a solution of the mixed boundary value problem (2.2), then

$$u = \frac{I}{\int_{\partial\mathcal{E}^+} \sigma \frac{\partial \tilde{u}}{\partial \mathbf{n}} \, ds} \tilde{u} \quad in \ \Omega \qquad (up \ to \ a \ constant). \tag{2.4}$$

Proof. The proof is elementary by looking at the energy of $w = u - c\tilde{u}$ for a constant c:

$$\begin{aligned}\int_\Omega \sigma|\nabla w|^2\,d\mathbf{r} &= \int_{\partial\Omega} \sigma\frac{\partial w}{\partial \mathbf{n}}\, w\, ds \\ &= \int_{\mathcal{E}^+} \sigma\frac{\partial w}{\partial \mathbf{n}}\, ds\, (u|_{\mathcal{E}^+} - c) \,+ \left(\int_{\mathcal{E}^-} \sigma\frac{\partial w}{\partial \mathbf{n}}\, ds\right)\, u|_{\mathcal{E}^-} \\ &= (u|_{\mathcal{E}^+} - u|_{\mathcal{E}^-} - c)\left(I \,- c\int_{\partial\mathcal{E}^+} \sigma\frac{\partial \tilde{u}}{\partial \mathbf{n}} ds\right).\end{aligned}$$

Hence, for $c = \frac{I}{\int_{\partial\mathcal{E}^+} \sigma\frac{\partial\tilde{u}}{\partial\mathbf{n}}\, ds}$, the above relation generates $|\nabla w| = 0$ in Ω, which means w is a constant in Ω. □

Now, we explain the inverse problem for the MREIT model, in which we try to reconstruct σ. The presence of the internal current density $\mathbf{J} = -\sigma\nabla u$ generates a magnetic flux density $\mathbf{B} = (B_x, B_y, B_z)$ such that the Ampere law $\mathbf{J} = \nabla\times\mathbf{B}/\mu_0$ holds in Ω. With z-axis pointing to the direction of the main magnetic field of the MRI scanner, the relation between the measurable quantity B_z and the unknown σ is governed by the Biot-Savart law:

$$B_z(\mathbf{r}) = \frac{\mu_0}{4\pi}\int_\Omega \frac{\langle \mathbf{r}-\mathbf{r}'\,,\ \sigma(\mathbf{r}')\mathbb{L}\nabla u(\mathbf{r}')\rangle}{|\mathbf{r}-\mathbf{r}'|^3}\, d\mathbf{r}' \qquad \text{for } \mathbf{r}\in\Omega, \tag{2.5}$$

where $\mathbb{L} = \begin{pmatrix} 0 & 1 & 0 \\ -1 & 0 & 0 \\ 0 & 0 & 0 \end{pmatrix}$. Here, we must read u as a nonlinear function of σ. The following lemma is crucial to understand why we need at least two injection currents with the requirement (2.11) in the sequel.

Lemma 2.2. *Suppose u is a solution of (2.2) and the pair (σ, u) satisfies (2.5). Then B_z in (2.5) can be expressed as*

$$B_z = \frac{\mu_0}{4\pi}\int_\Omega \frac{-1}{|\mathbf{r}-\mathbf{r}'|}\begin{vmatrix} \frac{\partial\sigma}{\partial x} & \frac{\partial\sigma}{\partial y} \\ \frac{\partial u}{\partial x} & \frac{\partial u}{\partial y}\end{vmatrix} d\mathbf{r}' + \frac{\mu_0}{4\pi}\int_{\partial\Omega}\frac{1}{|\mathbf{r}-\mathbf{r}'|}\,\mathbf{n}\cdot(\sigma\mathbb{L}\nabla u)\, ds. \tag{2.6}$$

Moreover, there exist infinitely many pairs $(\tilde{\sigma}, \tilde{u})$ such that $\begin{vmatrix} \frac{\partial\sigma}{\partial x} & \frac{\partial\sigma}{\partial y} \\ \frac{\partial u}{\partial x} & \frac{\partial u}{\partial y}\end{vmatrix} = \begin{vmatrix} \frac{\partial\tilde{\sigma}}{\partial x} & \frac{\partial\tilde{\sigma}}{\partial y} \\ \frac{\partial\tilde{u}}{\partial x} & \frac{\partial\tilde{u}}{\partial y}\end{vmatrix}$ *in Ω and $\mathbf{n}\cdot(\sigma\mathbb{L}\nabla u) = \mathbf{n}\cdot(\tilde{\sigma}\mathbb{L}\nabla\tilde{u})$ on $\partial\Omega$.*

Proof. From (2.5), we have

$$\begin{aligned} B_z &= \tfrac{\mu_0}{4\pi}\int_\Omega \nabla_{\mathbf{r}'}\tfrac{1}{|\mathbf{r}-\mathbf{r}'|}\cdot(\sigma(\mathbf{r}')\mathbb{L}\nabla u(\mathbf{r}'))\, d\mathbf{r}' \\ &= \tfrac{\mu_0}{4\pi}\int_\Omega \tfrac{-1}{|\mathbf{r}-\mathbf{r}'|}\nabla\cdot(\sigma\mathbb{L}\nabla u)\, d\mathbf{r}' + \tfrac{\mu_0}{4\pi}\int_{\partial\Omega}\tfrac{1}{|\mathbf{r}-\mathbf{r}'|}\,\mathbf{n}\cdot(\sigma\mathbb{L}\nabla u)\, ds.\end{aligned}$$

Then (2.6) follows from $\nabla\cdot(\sigma\mathbb{L}\nabla u) = \mathbf{e}_z\cdot[\nabla\sigma\times\nabla u] = \begin{vmatrix} \frac{\partial\sigma}{\partial x} & \frac{\partial\sigma}{\partial y} \\ \frac{\partial u}{\partial x} & \frac{\partial u}{\partial y}\end{vmatrix}$, where $\mathbf{e}_z = (0,0,1)$.

Now, we will show that there are infinitely many pairs $(\tilde{\sigma}, \tilde{u})$ such that $\mathbf{e}_z\cdot[\nabla\sigma\times\nabla u] = \mathbf{e}_z\cdot[\nabla\tilde{\sigma}\times\nabla\tilde{u}]$ and $\tilde{u}$ is a solution of (2.2) with σ replaced by $\tilde{\sigma}$. Indeed, we can construct infinitely many pairs $(\tilde{\sigma}, \tilde{u})$ satisfying the much stronger condition $\sigma\nabla u = \tilde{\sigma}\nabla\tilde{u}$. From the maximum-minimum principle for elliptic equation, $u|_{\mathcal{E}^+}$ and $u|_{\mathcal{E}^-}$ are the maximum and minimum values of u in $\overline{\Omega}$, respectively. Choose a and b such that $\inf_\Omega u = u|_{\mathcal{E}^-} < a < b < u|_{\mathcal{E}^+} = \sup_\Omega u$. For any increasing function $\phi\in C^2([a,b])$ satisfying

$$\phi'(a) = \phi'(b) = 1, \quad \phi''(a) = \phi''(b) = 0, \quad \phi(a) = a,\ \phi(b) = b, \tag{2.7}$$

we define

$$\tilde{u}(\mathbf{r}) = \begin{cases} \phi(u(\mathbf{r})) & \text{if } \mathbf{r}\in\hat{\Omega} \\ u(\mathbf{r}) & \text{if } \mathbf{r}\in\Omega\setminus\hat{\Omega}\end{cases}, \quad \tilde{\sigma}(\mathbf{r}) = \begin{cases} \frac{\sigma(\mathbf{r})}{\phi'(u(\mathbf{r}))} & \text{if } \mathbf{r}\in\hat{\Omega} \\ \sigma(\mathbf{r}) & \text{if } \mathbf{r}\in\Omega\setminus\hat{\Omega},\end{cases}$$

where $\hat{\Omega} := \{\mathbf{r} \in \Omega \ : \ a \le u(\mathbf{r}) \le b\}$. The conditions of ϕ guarantee $\tilde{\sigma} \in C^1(\Omega)$ and $\tilde{\sigma} > 0$ in Ω. Since $\nabla\tilde{u} = \phi'(u)\nabla u$, we have $\tilde{\sigma}\nabla\tilde{u} = \frac{\sigma}{\phi'(u)}\nabla\hat{u} = \sigma\nabla u$. So it is clear that $\begin{vmatrix} \frac{\partial\sigma}{\partial x} & \frac{\partial\sigma}{\partial y} \\ \frac{\partial u}{\partial x} & \frac{\partial u}{\partial y} \end{vmatrix} = \begin{vmatrix} \frac{\partial\tilde{\sigma}}{\partial x} & \frac{\partial\tilde{\sigma}}{\partial y} \\ \frac{\partial\tilde{u}}{\partial x} & \frac{\partial\tilde{u}}{\partial y} \end{vmatrix}$ and $\mathbf{n} \cdot (\sigma\mathbb{L}\nabla u) = \mathbf{n} \cdot (\tilde{\sigma}\mathbb{L}\nabla\tilde{u})$ on $\partial\Omega$. Since $\tilde{u} = u$ near the electrodes $\mathcal{E}^+$ and $\mathcal{E}^-$, $\tilde{u}$ has the same boundary condition on the electrodes as u. Therefore, $\tilde{u}$ is a solution of (2.2) with σ replaced by $\tilde{\sigma}$. This completes the proof since ϕ can be chosen arbitrarily under the constraint (2.7). □

According to Lemma 2.2, the unique determination of σ requires us to inject at least two input currents I_1 and I_2. Now, we are ready to explain the exact MREIT model. We inject electrical currents I_1 and I_2 through two pairs of surface electrodes $\mathcal{E}_1^{\pm}$ and $\mathcal{E}_2^{\pm}$, respectively. Let u_j and B_z^j be the potential and magnetic flux density corresponding to I_j with $j = 1, 2$.

For the measured data B_z^1, B_z^2 corresponding to two input currents I_1, I_2 and a given constant $\alpha > 0$, we try to reconstruct σ satisfying the following conditions for $j = 1, 2$:

$$\begin{cases} \nabla \cdot (\sigma\nabla u_j) = 0 \quad \text{in } \Omega \\ I = \int_{\mathcal{E}^+} \sigma\frac{\partial u_j}{\partial \mathbf{n}}\, ds = -\int_{\mathcal{E}^+} \sigma\frac{\partial u_j}{\partial \mathbf{n}}, \quad \nabla u_j \times \mathbf{n}|_{\mathcal{E}^+\cup\mathcal{E}^-} = 0 \\ \sigma\frac{\partial u_j}{\partial \mathbf{n}} = 0 \quad \text{on } \partial\Omega \setminus \overline{\mathcal{E}^+ \cup \mathcal{E}^-} \\ B_z^j(\mathbf{r}) = \frac{\mu_0}{4\pi}\int_\Omega \frac{\langle \mathbf{r}-\mathbf{r}',\, \sigma\mathbb{L}\nabla u_j\rangle}{|\mathbf{r}-\mathbf{r}'|^3}\, d\mathbf{r}', \quad \mathbf{r} \in \Omega \\ \left| u_1|_{\mathcal{E}_2^+} - u_1|_{\mathcal{E}_2^-} \right| = \alpha. \end{cases} \tag{2.8}$$

Remark 2.3. The last condition regarding α is necessary for fixing the scaling uncertainty of σ. Without this condition, whenever σ and u_j satisfy the other four relations in (2.8), so do $c\sigma$ and $\frac{u_j}{c}$ for any positive constant c. Here, we should avoid measuring the voltage difference between the pair of electrodes used for current injection since any electrode contact impedance may cause measurement errors. Therefore, in practice, we usually use the other pair of electrodes for the voltage measurement.

To explain the MREIT image reconstruction algorithm, we define

$$\mathcal{L}_{z_0}\sigma(x, y) := \sigma(x, y, z_0) + \frac{1}{2\pi}\int_{\partial\Omega_{z_0}} \frac{(x - x',\ y - y') \ \cdot \ \nu(x', y')}{|x - x'|^2 + |y - y'|^2}\, \sigma(x', y', z_0)\, dl, \tag{2.9}$$

where ν is the unit outward normal vector to $\partial\Omega_{z_0}$ and $\Omega_{z_0} := \Omega \cap \{z = z_0\} \subset \mathbb{R}^2$. For a vector-valued function $F = (F_1, F_2)$ defined on Ω, we define

$$\mathcal{G}_{z_0} * F(x, y) := \frac{1}{2\pi\mu_0}\int_{\Omega_{z_0}} \frac{(x - x',\ y - y')}{|x - x'|^2 + |y - y'|^2} \cdot F(x', y', z_0)\, dx'dy'. \tag{2.10}$$

Let $u_j[\sigma]$ be a solution to the direct problem (2.2) corresponding to I_j satisfying

$$\begin{vmatrix} \frac{\partial u_1}{\partial x} & \frac{\partial u_1}{\partial y} \\ \frac{\partial u_2}{\partial x} & \frac{\partial u_2}{\partial y} \end{vmatrix} \neq 0 \quad \text{in } \Omega \tag{2.11}$$

and set

$$\mathbb{A}[\sigma] := \begin{bmatrix} \frac{\partial u_1[\sigma]}{\partial y} & -\frac{\partial u_1[\sigma]}{\partial x} \\ \frac{\partial u_2[\sigma]}{\partial y} & -\frac{\partial u_2[\sigma]}{\partial x} \end{bmatrix}. \tag{2.12}$$

Now let us state the implicit relation between σ and B_z^j, on which the harmonic B_z algorithm is based.

Lemma 2.4. *Suppose that $|\nabla\sigma|$ is compactly supported in Ω and $u_j[\sigma]$ for $j = 1, 2$ satisfy (2.11). Then the following identity*

$$\mathcal{L}_z\sigma(x,y) = \mathcal{G}_z * \left(\mathbb{A}[\sigma]^{-1} \begin{bmatrix} \nabla^2 B_z^1 \\ \nabla^2 B_z^2 \end{bmatrix} \right)(x,y), \qquad (x,y) \in \Omega_z \tag{2.13}$$

holds for each z. Moreover, $\mathcal{L}_z : H_*^{1/2}(\Omega_z) \to H_*^{1/2}(\Omega_z)$ is invertible where $H_*^{1/2}(\Omega_z) := \{\eta \in H^{1/2}(\Omega_z) : \int_{\partial\Omega_z} \eta = 0\}$.

Proof. The proof of (2.13) is based on the fact that $\nabla \cdot \mathbf{B} = 0$ and the Ampere law $\mathbf{J} = \frac{1}{\mu_0}\nabla \times \mathbf{B}$. Direct computation yields $\nabla u_j \times \nabla\sigma = \frac{1}{\mu_0}\Delta\mathbf{B}^j$ and we have

$$\begin{bmatrix} \frac{\partial\sigma}{\partial x} \\ \frac{\partial\sigma}{\partial y} \end{bmatrix} = \frac{1}{\mu_0}\mathbb{A}[\sigma]^{-1} \begin{bmatrix} \Delta B_z^1 \\ \Delta B_z^2 \end{bmatrix}. \tag{2.14}$$

Since $\nabla\sigma = 0$ near $\partial\Omega$, so does $\Delta B_z = 0$. Hence, the right-hand side of (2.13) is well defined. Now, the result follows from the formal identity

$$\sigma(x,y,z) = \int_{\Omega_z} \frac{1}{2\pi}\left(\frac{\partial^2}{\partial x^2} + \frac{\partial^2}{\partial y^2}\right) \log\sqrt{(x-x')^2 + (y-y')^2}\,\sigma(x',y',z)dx'dy'$$

and integration by parts.

The invertibility of $\mathcal{L}$ can be proven by the standard layer potential theory [9, 24]. Let $w \in H_*^{1/2}(\Omega_z)$. We will find $v \in H_*^{1/2}(\Omega_z)$ such that $\mathcal{L}_z v = w$. Note that $w|_{\partial\Omega_z} \in L_*^2(\partial\Omega_z) := \{\phi \in L^2(\Omega_z) : \int_{\partial\Omega_z} \phi = 0\}$. It is well known that there exists a unique $\psi \in L_*^2(\partial\Omega_z)$ such that $\frac{1}{2}\psi - \mathcal{K}\psi = w|_{\partial\Omega_z}$ on $\partial\Omega_z$ where $\mathcal{K}\psi(x,y) = \frac{-1}{2\pi}\int_{\partial\Omega_{z_0}} \frac{(x-x',\, y-y')\cdot\nu}{|x-x'|^2+|y-y'|^2}\ \psi(x',y')\ dl$ for $(x,y) \in \partial\Omega_z$. Now, we define

$$v(x,y) = w(x,y) - \frac{1}{2\pi}\int_{\partial\Omega_{z_0}} \frac{(x-x',\ y-y')\ \cdot\ \nu(x',y')}{|x-x'|^2 + |y-y'|^2}\ \psi(x',y')\ dl \tag{2.15}$$

for $(x,y) \in \Omega_z$. Due to the trace formula of the double layer potential, $v = \psi$ on $\partial\Omega_z$. By replacing ψ in (2.15) with v, we have $w = \mathcal{L}_z v$ and this completes the proof. □

Remark 2.5. The condition (2.11) is necessary for the harmonic B_z algorithm. However, we still do not have a rigorous theory for the issue related to (2.11) in a three-dimensional domain. In the two-dimensional case, the validity of condition (2.11), under suitably chosen boundary data, is proven in [4] when σ is smooth. When σ is just measurable, (2.11) holds in the *a.e. sense* [3]. In the 3-D case there are examples [5, 13] which suggest that it may be difficult, if not impossible, to find boundary data such that (2.11) holds independently of σ, even assuming smoothness of σ.

In this paper, we will consider the convergence result for the harmonic B_z method based on the governed problem (2.3), since the solution u to the standard governed problem (2.2) can be expressed as a constant multiple in terms of Lemma 2.1. Let σ^* be the target conductivity to be determined. Based on Lemma 2.4, the harmonic B_z algorithm approximating σ^* at each slice Ω_{z_0}, for given σ^* on $\partial\Omega_{z_0}$, can be stated as follows. Notice, here we also use σ^* to represent the known boundary value of unknown conductivity σ^* defined in the whole domain, which can be distinguished from the context. Given an initial guess

$\sigma^0(x,y,z)$ in Ω with exact boundary values, the harmonic B_z iteration algorithm constructs an approximation sequence $\{\sigma^n(x,y,z_0)\}$ by

$$\begin{cases} \nabla\sigma^{n+1}(x,y,z_0) := \frac{1}{\mu_0}\mathbb{A}[\sigma^n]^{-1}\begin{bmatrix} \Delta B_z^1 \\ \Delta B_z^2 \end{bmatrix} \\ \sigma^{n+1}(x,y,z_0) := H(\sigma^*) - \frac{1}{2\pi}\int_{\Omega_{z_0}} \frac{(x-x'\ ,\ y-y')}{|x-x'|^2+|y-y'|^2}\ \cdot\nabla\sigma^{n+1}(x',y',z_0)dx'dy' \end{cases} \tag{2.16}$$

for $n = 0, 1, 2, \cdots$ at each slice Ω_{z_0}, where $\mathbb{A}[\sigma]$ is defined in (2.12) and

$$H(\sigma^*) := \frac{1}{2\pi}\int_{\partial\Omega_{z_0}} \frac{(x-x'\ ,\ y-y')\ \cdot\ \nu(x',y')}{|x-x'|^2+|y-y'|^2}\ \sigma^*(x',y',z_0)\ dl.$$

Notice that, to compute $\mathbb{A}[\sigma^n]^{-1}$ at each slice $\Omega_{z_0} \subset \mathbb{R}^2$, we need the value σ^n in the whole domain $\Omega \subset \mathbb{R}^3$. This fact will cause some difficulties when we do the iteration for the full three-dimensional model (see the convergence proof in subsection 3.2 of this paper). On the other hand, in the above scheme, the value of σ^n on the boundary of the slice Ω_{z_0} is specified as the exact value $\sigma^*(x,y,z_0)$ for all n.

3 Convergence for harmonic B_z algorithm

It should be noticed that $\mathbb{A}[\sigma^n]^{-1}(x,y,z)$ may be large near $\partial\Omega$ due to the fact that two induced currents $\sigma^n\nabla u_1^n, \sigma^n\nabla u_2^n$ are probably almost parallel for some configuration. To avoid this case, let us assume that σ^* is constant in $\Omega\setminus\tilde{\Omega}$ for some interior domain $\tilde{\Omega}$. Then it is easy to show that $\nabla^2 B_z^1 \equiv \nabla^2 B_z^2 \equiv 0$ in $\Omega\setminus\tilde{\Omega}$. So the original iteration scheme (2.16) at each slice becomes

$$\begin{cases} \nabla\sigma^{n+1}(x,y,z_0) := \frac{1}{\mu_0}\mathbb{A}[\sigma^n]^{-1}\begin{bmatrix} \Delta B_z^1 \\ \Delta B_z^2 \end{bmatrix}, \\ \sigma^{n+1}(x,y,z_0) := \tilde{H}(\sigma^*) - \frac{1}{2\pi}\int_{\tilde{\Omega}_{z_0}} \frac{(x-x'\ ,\ y-y')}{|x-x'|^2+|y-y'|^2}\ \cdot\nabla\sigma^{n+1}(x',y',z_0)dx'dy' \end{cases} \tag{3.1}$$

for $(x,y) \in \tilde{\Omega}_{z_0}$, where $\tilde{\Omega}_{z_0} = \tilde{\Omega}\bigcap\{(x,y,z) : z = z_0\} \subset \mathbb{R}^2$ and $\tilde{H}(\sigma^*)$ is $H(\sigma^*)$ with $\partial\Omega_{z_0}$ replaced by $\partial\tilde{\Omega}_{z_0}$. For $(x,y) \in \Omega_{z_0}\setminus\tilde{\Omega}_{z_0}$, it is obvious that $\sigma^n(x,y,z_0) \equiv \sigma^*(x,y,z_0)$ from this iteration since $\nabla\sigma^n \equiv 0$ in $\Omega_{z_0}\setminus\tilde{\Omega}_{z_0}$.

The major difficulty dealing with the convergence comes from the uniform upper bound of the inverse matrix $\mathbb{A}[\sigma^n]^{-1}$ in the iteration procedure. Without some uniform bound on the iteration conductivity σ^n, it is quite difficult to estimate $\mathbb{A}[\sigma^n]^{-1}$. The key taken in this paper to overcome this difficulty is some assumptions on the target conductivity and the initial guess. With these conditions, we can establish the convergence. Rather than the general way of the convergence proof which sets the uniform bound for the sequence $\{\sigma^n\}$ and then obtains the convergence of the sequence, we should establish the uniform bound on σ^n and estimate the error $\|\sigma^n - \sigma^*\|$ at each step simultaneously by the induction argument.

We first give the following estimates, which will be used in the convergence proof.

Lemma 3.1. *Denote by $\mathcal{E}$ any regular open subsurface of the boundary $\partial\Omega$ of $\Omega \subset \mathbb{R}^m$ with $m = 2, 3$. Then for the boundary value problem*

$$\begin{cases} \nabla\cdot(\sigma\nabla u) = \nabla\cdot f & \text{in } \Omega \\ u|_{\mathcal{E}} = h & \text{on } \mathcal{E} \\ -\sigma\nabla u\cdot\ \mathbf{n} = g & \text{on } \partial\Omega\setminus\overline{\mathcal{E}} \end{cases} \tag{3.2}$$

with $\sigma \in L^\infty(\Omega)$ *satisfying* $\inf_\Omega \sigma > 0$ *and* $h \in H^{1/2}(\mathcal{E})$, $g \in H^{-1/2}(\partial\Omega \setminus \overline{\mathcal{E}})$, *the following estimates hold:*

If $f \in (L^2(\Omega))^m$ *and* $\sigma \in C(\Omega)$, *then* $u \in H^1(\Omega)$ *and satisfies*

$$\|u\|_{H^1(\Omega)} \leq C_1(\sigma)[\|f\|_{L^2(\Omega)} + \|h\|_{H^{1/2}(\mathcal{E})} + \|g\|_{H^{-1/2}(\partial\Omega\setminus\overline{\mathcal{E}})}]; \tag{3.3}$$

If $f \in (H^1(\Omega))^m$ *and* $\sigma \in C^1(\Omega)$, *then* $u \in H^2(\tilde{\Omega})$ *and*

$$\|u\|_{H^2(\tilde{\Omega})} \leq C_2(\sigma)[\|u\|_{H^1(\Omega)} + \|\nabla \cdot f\|_{L^2(\Omega)}]; \tag{3.4}$$

If $f \in (C^{0,\alpha}(\Omega))^m$ *with* $\alpha \in (0,1)$ *and* $\sigma \in C^1(\Omega)$, *then* $u \in C^{1,\alpha}(\tilde{\tilde{\Omega}})$ *and*

$$\|\nabla u\|_{C^{0,\alpha}(\tilde{\Omega})} \leq C_3(\sigma)[\|u\|_{C^{0,\alpha}(\tilde{\tilde{\Omega}})} + \|f\|_{C^{0,\alpha}(\tilde{\tilde{\Omega}})}]; \tag{3.5}$$

If $f \in (L^p(\Omega))^m$ *with* $p > 1$ *and* $\sigma \in C(\Omega)$, *then* $u \in W^{1,p}(\tilde{\tilde{\Omega}})$ *and*

$$\|\nabla u\|_{L^p(\tilde{\Omega})} \leq C_4(\sigma)[\|u\|_{L^p(\tilde{\tilde{\Omega}})} + \|f\|_{L^p(\tilde{\tilde{\Omega}})}], \tag{3.6}$$

where $\tilde{\Omega} \subset\subset \tilde{\tilde{\Omega}} \subset\subset \Omega$ *are regular domains, and the functions* $C_i(\sigma)$ *have the following forms:*

$$C_i(\sigma) = F_i(\|\sigma\|_{C(\Omega)}, \|\nabla\sigma\|_{C(\Omega)}, \frac{1}{\inf_\Omega \sigma}), \quad i = 2, 3, \tag{3.7}$$

$$C_i(\sigma) = F_i(\|\sigma\|_{C(\Omega)}, \frac{1}{\inf_\Omega \sigma}), \quad i = 1, 4. \tag{3.8}$$

The functions F_i $(i = 1, 2, 3, 4)$ *are known bounded functions with respect to the arguments.*

For the proof of these estimates, we refer to [8] and Theorem 8.8, Theorem 8.32 and Corollary 8.36 in [10]. The form of the constant $C_i(\sigma)$ is of importance in our convergence proof.

3.1 Convergence in axially symmetric cylindrical sections

Let $\Omega := D \times \mathbb{R}^1 \subset \mathbb{R}^3$ be a cylinder along z direction with infinite length and the fixed cross section $D \subset \mathbb{R}^2$. We assume that the conductivity σ^* in Ω does not change along z direction. That is, $\sigma^*(x, y, z) \equiv \sigma^*(x, y)$, $(x, y) \in D$.

Consider the electrodes $\mathcal{E}^\pm$ on $\partial\Omega$ where the input currents are specified. For an ideal electrode pair $\mathcal{E}^\pm$ parallel to z direction with infinite length, we assume that the current density is independent of z, see Figure 3. In this case, it follows from (2.2) that the potential u is also independent of z in Ω due to the causality and $u(x, y)$ meets

$$\begin{cases} \nabla \cdot (\sigma \nabla u) = 0 \quad \text{in } D \\ \tilde{I} = \int_{E^+} \sigma \frac{\partial u}{\partial \mathbf{n}}\, ds = -\int_{E^-} \sigma \frac{\partial u}{\partial \mathbf{n}} ds, \quad \nabla u \times \mathbf{n} = 0 \ \text{ on } E^+ \cup E^- \\ \sigma \frac{\partial u}{\partial \mathbf{n}} = 0 \quad \text{on } \partial\Omega \setminus \overline{E^+ \cup E^-} \end{cases} \tag{3.9}$$

where $E^\pm := \mathcal{E}^\pm \bigcap \overline{D} \subset \partial D$, $\tilde{I}$ the total input current in $E^\pm$, and $\mathbf{n} \in \mathbb{R}^2$ the outward normal direction of ∂D. The equation (3.9) is the governed model for potential $u(x, y)$, which is in fact defined in the two-dimensional domain D.

To unify the notations in our proof for convergence in both axially cylindrical case and three-dimensional case, we will use $\Omega, \mathcal{E}^\pm$ to represent the geometry in (3.9) instead of $D, E^\pm$ in this subsection. Now we can state our convergence result of the harmonic B_z method based on the model (3.9) for the two-dimensional domain $\Omega \subset \mathbb{R}^2$.

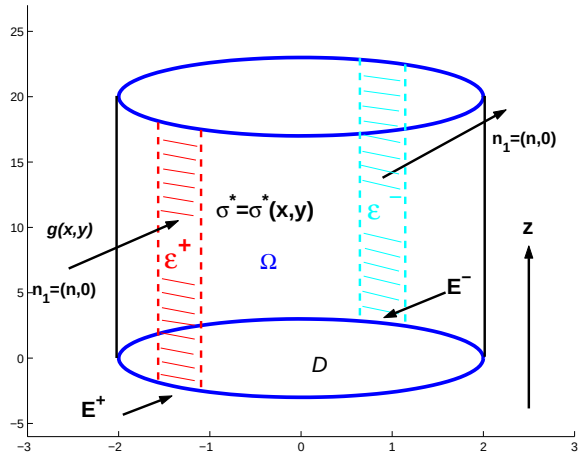

Figure 3: Axially symmetric cylindrical configuration.

Theorem 3.2. *Assume that the target conductivity* $\sigma^*(x,y) \in C^1(\overline{\Omega})$ *meets:*

H1. $0 < \sigma_-^* \le \sigma^*(x) \le \sigma_+^*$ *for known constants* $\sigma_\pm^*$*;*

H2. there exists $\tilde{\Omega} \subset\subset \Omega$ *such that* σ^* *is a known constant in* $\Omega \setminus \tilde{\Omega}$*;*

H3. $|\det A[\sigma^*](x,y)| \ge d_-^* > 0$ *in* $\tilde{\Omega}$ *where* d_-^* *is a known constant.*

Under these hypotheses, there exist constants $\epsilon = \epsilon(\sigma_\pm^*, d_-^*) > 0$ *small enough and* $\theta = \theta(\epsilon, \sigma_\pm^*, d_-^*) \in (0,1)$ *such that if we take the initial guess* σ^0 *as the constant* $\sigma^*|_{\Omega\setminus\tilde{\Omega}}$*, then the sequence* $\{\sigma^n\}$ *given by the harmonic* B_z *iteration scheme holds for* $\|\nabla\sigma^*\|_{C(\tilde{\Omega})} \le \epsilon$ *that*

$$\sigma^n \equiv \sigma^* \text{ in } \Omega\setminus\tilde{\Omega}, \quad \|\sigma^n - \sigma^*\|_{C^1(\tilde{\Omega})} \le K\theta^n\epsilon, \quad n = 1,2,\cdots \tag{3.10}$$

where $K := diam(\Omega) + 1$.

Remark 3.3. We obtain a local convergence for the target conductivity σ^* with small contrast. At present stage, we do not know how to remove the smallness requirement on ϵ.

Remark 3.4. The convergence property holds only in the interior domain $\tilde{\Omega}$. The reason is as follows. First, the regularity property of elliptic equation with mixed boundary condition will fail at the boundary. Second, for some geometry configuration, the induced internal currents near the boundary should be almost parallel, so it is very hard to get the uniform bound on $\mathbb{A}[\sigma^n]^{-1}$ near the boundary.

Proof. Let us take $0 < \epsilon < \frac{1}{2K}\sigma_-^*$. Denote by u_j^n and u_j^* the solutions of the direct problem

$$\begin{cases} \nabla\cdot(\sigma\nabla u_j) = 0, \quad \text{in} \quad \Omega \\ u_j|_{\mathcal{E}_j^+} = 1, \qquad u_j|_{\mathcal{E}_j^-} = 0 \\ -\sigma\nabla u_j \cdot \mathbf{n} = 0 \quad \text{on} \quad \partial\Omega \setminus \mathcal{E}_j^+ \cup \mathcal{E}_j^- \end{cases} \tag{3.11}$$

with $\sigma = \sigma^n$ and σ^*, respectively. This is a special case of (3.2) with $\mathcal{E} := \mathcal{E}_j^+ \bigcup \mathcal{E}_j^-$ in Lemma 3.1. For a given interior domain $\tilde{\Omega}$, there exists a constant $\overline{C}_* = \overline{C}_*(\sigma_\pm^*)$ such that

$$\left\|\nabla u_j^*\right\|_{C(\tilde{\Omega})} + \left\|u_j^*\right\|_{H^2(\tilde{\Omega})} \le \overline{C}_*. \tag{3.12}$$

This fact can be deduced from Lemma 3.1 as follows. Indeed, from the first and second points of this Lemma, we have $\left\|u_j^*\right\|_{H^2(\tilde{\tilde{\Omega}})} \leq C_1(\sigma^*)C_2(\sigma^*)$. By the Sobolev imbedding theorem, we have $\left\|u_j^*\right\|_{C^{0,\alpha}(\tilde{\tilde{\Omega}})} \leq C_s \left\|u_j^*\right\|_{H^2(\tilde{\tilde{\Omega}})}$ for every $\alpha \in (0,1)$. Finally, combining these last two estimates with the third point of Lemma 3.1, we have

$$\left\|\nabla u_j^*\right\|_{C(\tilde{\Omega})} + \left\|u_j^*\right\|_{H^2(\tilde{\Omega})} \leq C_s C_1(\sigma^*)C_2(\sigma^*)C_3(\sigma^*),$$

which leads to (3.12) with

$$\overline{C}_* := C_s \sup_{(t_1,t_2,t_3)\in\mathbb{S}_1} F_1(t_1,t_3)F_2(t_1,t_2,t_3)F_3(t_1,t_2,t_3), \tag{3.13}$$

where $\mathbb{S}_1 := [\sigma_-^*, \sigma_+^*] \times [0, \frac{1}{2K}\sigma_-^*] \times [\frac{1}{\sigma_+^*}, \frac{1}{\sigma_-^*}]$ and F_i are uniformly bounded with respect to their arguments.

Step 1: Expand the initial guess σ^0 at σ^*.

Expand σ^0 as $\sigma^0 = \sigma^* + e^0$. Since $\|\nabla\sigma^*\|_{C(\Omega)} < \epsilon$ and $\sigma^* = \sigma^0$ in $\Omega \setminus \tilde{\Omega}$,

$$\left\|e^0\right\|_{C(\Omega)} \leq diam(\Omega)| \left\|\nabla e^0\right\|_{C(\Omega)} \leq diam(\Omega)\epsilon.$$

Hence, $\left\|e^0\right\|_{C^1(\Omega)} \leq (diam(\Omega)+1)\epsilon = K\epsilon$. We expand u_j^0 at u_j^* as

$$u_j^0 = u_j^* + \epsilon w_j^0. \tag{3.14}$$

Noticing that $\sigma^0 = \sigma^*$ in $\Omega \setminus \tilde{\Omega}$, then ϵw_j^0 meets

$$\begin{cases} \nabla \cdot \left(\sigma^0 \nabla \epsilon w_j^0\right) = -\nabla \cdot (e^0 \nabla u_j^*) \quad \text{in} \quad \Omega \\ \epsilon w_j^0|_{\mathcal{E}_j^+} = 0, \qquad \epsilon w_j^0|_{\mathcal{E}_j^-} = 0 \\ -\sigma^0 \nabla \epsilon w_j^0 \cdot \ \mathbf{n} = (\sigma^0 - \sigma^*)\nabla u_j^* \cdot \ \mathbf{n} = 0 \quad \text{on} \quad \partial\Omega \setminus \mathcal{E}_j^+ \cup \mathcal{E}_j^-. \end{cases} \tag{3.15}$$

Since $\|e^0\|_{C^1(\tilde{\Omega})} \leq K\epsilon$ and $e^0 = 0$ in $\Omega \setminus \tilde{\Omega}$, it follows from (3.12) that the right-hand side of the first equation in (3.15) satisfies

$$\left\|\nabla \cdot (e^0 \nabla u_j^*)\right\|_{L^2(\Omega)} \leq \overline{C}_* \left\|e^0\right\|_{C^1(\tilde{\Omega})}. \tag{3.16}$$

Therefore it follows from Lemma 3.1 and the Sobolev imbedding theorem that

$$\begin{aligned} \left\|\epsilon w_j^0\right\|_{C(\tilde{\tilde{\Omega}})} &\leq C_s \left\|\epsilon w_j^0\right\|_{H^2(\tilde{\tilde{\Omega}})} \leq C_s C_2(\sigma^0)[\left\|\epsilon w_j^0\right\|_{H^1(\tilde{\Omega})} + \left\|\nabla \cdot e^0 \nabla u_j^*\right\|_{L^2(\tilde{\Omega})}] \\ &\leq C_s C_2(\sigma^0)[C_1(\sigma^0) \left\|e^0 \nabla u_j^*\right\|_{L^2(\Omega)} + \overline{C}_* \left\|e^0\right\|_{C^1(\Omega)}] \\ &\leq C_s C_2(\sigma^0)[C_1(\sigma^0)C_1(\sigma^*) + \overline{C}_*] \left\|e^0\right\|_{C^1(\Omega)}. \end{aligned}$$

Hence

$$\begin{aligned} \left\|\epsilon \nabla w_j^0\right\|_{C(\tilde{\Omega})} &\leq C_3(\sigma^0)[\left\|\epsilon w_j^0\right\|_{C(\tilde{\tilde{\Omega}})} + \left\|e^0 \nabla u_j^*\right\|_{C(\tilde{\Omega})}] \\ &\leq C_3(\sigma^0)[C_s C_2(\sigma^0)[C_1(\sigma^0)C_1(\sigma^*) + \overline{C}_*] + \overline{C}_*] \left\|e^0\right\|_{C^1(\Omega)}. \end{aligned} \tag{3.17}$$

We denote by

$$\overline{F}(\sigma) := C_3(\sigma) \left[C_s C_2(\sigma) \left(C_1(\sigma) \sup_{[\sigma_-^*, \sigma_+^*] \times [\frac{1}{\sigma_+^*}, \frac{1}{\sigma_-^*}]} F_1(t_1,t_3) + \overline{C}_* \right) + \overline{C}_* \right], \tag{3.18}$$

a known function due to the Lemma 3.1. For $\epsilon \in (0, \frac{1}{2K}\sigma_-^*)$, we introduce the constant

$$\overline{C}_\epsilon(\sigma^*) := \sup_{\|\sigma-\sigma^*\|_{C^1(\Omega)} \le K\epsilon} \overline{F}(\sigma), \tag{3.19}$$

which is well-defined. Noticing that $\|\sigma - \sigma^*\|_{C^1(\Omega)} \le K\epsilon$, we have $\sigma > \frac{1}{2}\sigma_-^* > 0$ for $0 < \epsilon < \frac{1}{2K}\sigma_-^*$ due to H1. Moreover, this constant can be estimated by a known constant as

$$\overline{C}_\epsilon(\sigma^*) \le \sup_{\mathbb{S}_2} \overline{F}(\sigma) =: \overline{G}(\sigma_\pm^*) \tag{3.20}$$

for $\epsilon \in (0, \frac{1}{2K}\sigma_-^*)$ from the *a priori* information about σ^*, where

$$\mathbb{S}_2 := \left\{ \sigma(x,y) : \frac{1}{2}\sigma_-^* < \sigma < \frac{1}{2}\sigma_-^* + \sigma_+^*,\ \|\nabla\sigma\|_C \le \frac{K+1}{2K}\sigma_-^* \right\}.$$

Now it follows from (3.17), (3.18), (3.19) and (3.20) that

$$\left\|\epsilon\nabla w_j^0\right\|_{C(\tilde{\Omega})} \le \overline{G}(\sigma_\pm^*) \left\|e^0\right\|_{C^1(\Omega)}. \tag{3.21}$$

Since $\|e^0\|_{C^1(\tilde{\Omega})} \le K\epsilon$, it follows that

$$\left\|\nabla w_j^0\right\|_{C(\tilde{\Omega})} \le K\overline{G}(\sigma_\pm^*). \tag{3.22}$$

Step 2. Estimate $\left\|\sigma^1 - \sigma^*\right\|_{C^1(\tilde{\Omega})}$.

First, $\mathbb{A}[\sigma^*]^{-1}$ exists from H3. From the definition, we know that $\nabla\sigma^1$ satisfies

$$\mathbb{A}[\sigma^0]\nabla\sigma^1 = \frac{1}{\mu_0}\begin{bmatrix} \Delta B_z^1 \\ \Delta B_z^2 \end{bmatrix},$$

which can be written as

$$\left(I + \epsilon\mathbb{A}[\sigma^*]^{-1}\begin{bmatrix} \frac{\partial w_1^0}{\partial y}, & -\frac{\partial w_1^0}{\partial x} \\ \frac{\partial w_2^0}{\partial y}, & -\frac{\partial w_2^0}{\partial x} \end{bmatrix}\right)\nabla\sigma^1 = \frac{1}{\mu_0}\mathbb{A}[\sigma^*]^{-1}\begin{bmatrix} \Delta B_z^1 \\ \Delta B_z^2 \end{bmatrix} = \nabla\sigma^*$$

due to the definition of the matrix $\mathbb{A}[\sigma^0]$ and (3.14). So we have

$$\left(I + \epsilon\mathbb{A}[\sigma^*]^{-1}\begin{bmatrix} \frac{\partial w_1^0}{\partial y}, & -\frac{\partial w_1^0}{\partial x} \\ \frac{\partial w_2^0}{\partial y}, & -\frac{\partial w_2^0}{\partial x} \end{bmatrix}\right)\nabla(\sigma^1 - \sigma^*) = -\epsilon\mathbb{A}[\sigma^*]^{-1}\begin{bmatrix} \frac{\partial w_1^0}{\partial y}, & -\frac{\partial w_1^0}{\partial x} \\ \frac{\partial w_2^0}{\partial y}, & -\frac{\partial w_2^0}{\partial x} \end{bmatrix}\nabla\sigma^*. \tag{3.23}$$

On the other hand, it is obvious from (3.22) that

$$\begin{aligned} \left\|\epsilon\mathbb{A}[\sigma^*]^{-1}\begin{bmatrix} \frac{\partial w_1^0}{\partial y}, & -\frac{\partial w_1^0}{\partial x} \\ \frac{\partial w_2^0}{\partial y}, & -\frac{\partial w_2^0}{\partial x} \end{bmatrix}\right\|_{C(\tilde{\Omega})} &\le \epsilon\left\|\mathbb{A}[\sigma^*]^{-1}\right\|_{C(\tilde{\Omega})}\sqrt{2}\max_{j=1,2}\left\|\nabla w_j^0\right\|_{C(\tilde{\Omega})} \\ &\le \epsilon\left\|\mathbb{A}[\sigma^*]^{-1}\right\|_{C(\tilde{\Omega})}\sqrt{2}\overline{G}(\sigma_\pm^*)K. \end{aligned} \tag{3.24}$$

A direct computation leads to $\left\|\mathbb{A}[\sigma^*]^{-1}\right\|_{C(\tilde{\Omega})} \le \frac{\sqrt{2}}{d_-^*}\max_{j=1,2}\|\nabla u_j(\sigma^*)\|_{C(\tilde{\Omega})}$, from which we deduce

$$\left\|\mathbb{A}[\sigma^*]^{-1}\right\|_{C(\tilde{\Omega})} \le \frac{\sqrt{2}}{d_-^*}\overline{C}_* \tag{3.25}$$

due to (3.12). Now we take $\epsilon \in (0, \frac{1}{2K}\sigma_-^*)$ small enough such that

$$\epsilon \frac{2}{d_-^*}\overline{G}(\sigma_\pm^*)\overline{C}_* K < \frac{1}{2}, \tag{3.26}$$

then it follows from (3.25) that

$$\epsilon \left\|\mathbb{A}[\sigma^*]^{-1}\right\|_{C(\tilde{\Omega})} \sqrt{2}\overline{G}(\sigma_\pm^*)K < \frac{1}{2}. \tag{3.27}$$

It follows from (3.22), (3.23) and (3.27) that

$$\begin{aligned} \left\|\nabla(\sigma^1 - \sigma^*)\right\|_{C(\tilde{\Omega})} &\leq 2\epsilon \left\|\mathbb{A}[\sigma^*]^{-1}\right\|_{C(\tilde{\Omega})} \sqrt{2} \max_{j=1,2} \left\|\nabla w_j^0\right\| \|\nabla\sigma^*\|_{C(\tilde{\Omega})} \\ &\leq 2\sqrt{2} \left\|\mathbb{A}[\sigma^*]^{-1}\right\|_{C(\tilde{\Omega})} \overline{G}(\sigma_\pm^*)K\epsilon^2. \end{aligned} \tag{3.28}$$

This last estimate generates

$$\left\|\sigma^1 - \sigma^*\right\|_{C^1(\tilde{\Omega})} \leq K \left\|\nabla(\sigma^1 - \sigma^*)\right\|_{C(\tilde{\Omega})} \leq K2\sqrt{2} \left\|\mathbb{A}[\sigma^*]^{-1}\right\|_{C(\tilde{\Omega})} \overline{G}(\sigma_\pm^*)K\epsilon^2.$$

Introducing a new constant

$$\overline{D}_* := K\frac{4}{d_-^*}\overline{C}_*, \tag{3.29}$$

the above estimate becomes

$$\left\|\sigma^1 - \sigma^*\right\|_{C^1(\tilde{\Omega})} \leq \overline{D}_*\overline{G}(\sigma_\pm^*)K\epsilon^2 \tag{3.30}$$

due to (3.25). For $\epsilon \in (0, \frac{1}{2K}\sigma_-^*)$ satisfying (3.26), it follows from the definition of $\overline{D}_*$ that

$$\epsilon\overline{D}_*\overline{G}(\sigma_\pm^*) := \theta \in (0,1) \tag{3.31}$$

and then

$$\left\|\sigma^1 - \sigma^*\right\|_{C^1(\tilde{\Omega})} \leq K\theta\epsilon, \tag{3.32}$$

which implies via (3.19) that

$$\overline{F}(\sigma^1) \leq \overline{C}_\epsilon(\sigma^*). \tag{3.33}$$

From (3.26) and (3.31), we assert that $\epsilon := \epsilon(\sigma_\pm^*, d_-^*)$ and $\theta := \theta(\epsilon, \sigma_\pm^*, d_-^*)$. Since σ^* is constant in $\Omega \setminus \tilde{\Omega}$, then we deduce from (2.14) that $\nabla^2 B_z^j = 0$ in $\Omega \setminus \tilde{\Omega}$, $j = 1, 2$. Hence from (2.16) we deduce that $\nabla\sigma^1 = 0$ in $\Omega \setminus \tilde{\Omega}$ and therefore $\sigma^1 = \sigma^*$ in $\Omega \setminus \tilde{\Omega}$, since $\sigma^1 = \sigma^*$ on $\partial\Omega$. Now, we can apply the induction argument to prove the theorem. That is, assume that the following properties

$$\left\|\sigma^k - \sigma^*\right\|_{C^1(\tilde{\Omega})} \leq K\theta^k\epsilon, \text{ and } \sigma^k = \sigma^* \text{ in } \Omega \setminus \tilde{\Omega} \tag{3.34}$$

are true for $k = n$. We shall prove that it is also true for $k = n + 1$.

Step 3. Expand σ^n at σ^*.

For the expansion $\sigma^n = \sigma^* + e^n$, it follows that

$$\|e^n\|_{C^1(\tilde{\Omega})} \leq (\overline{D}_*\overline{G}(\sigma_\pm^*))^n K\epsilon^{n+1} \tag{3.35}$$

from (3.34) with $k = n$. Correspondingly, we expand the solution u_j^n at u_j^* as

$$u_j^n = u_j^* + \epsilon^{n+1} w_j^n. \tag{3.36}$$

Noticing $\sigma^n = \sigma^*$ in $\Omega \setminus \tilde{\Omega}$, it is easy to see that $\epsilon^{n+1} w_j^n$ satisfies

$$\begin{cases} \nabla \cdot \left(\sigma^n \nabla \epsilon^{n+1} w_j^n\right) = -\nabla \cdot (e^n \nabla u_j^*) \quad \text{in} \quad \Omega, \\ \epsilon^{n+1} w_j^n|_{\mathcal{E}_j^+} = 0, \qquad \epsilon^{n+1} w_j^n|_{\mathcal{E}_j^-} = 0, \\ -\sigma^n \nabla \epsilon^{n+1} w_j^n \cdot \ \mathbf{n} = (\sigma^n - \sigma^*) \nabla u_j^* \cdot \ \mathbf{n} = 0 \quad \text{on} \quad \partial\Omega \setminus \mathcal{E}_j^+ \cup \mathcal{E}_j^-. \end{cases} \tag{3.37}$$

Similarly as in (3.21), we have

$$\left\|\nabla \epsilon^{n+1} w_j^n\right\|_{C(\tilde{\Omega})} \le \overline{F}(\sigma^n) \left\|e^n\right\|_{C^1(\Omega)} \le \overline{F}(\sigma^n)(\overline{D}_* \overline{G}(\sigma_\pm^*))^n K \epsilon^{n+1}.$$

That is,

$$\left\|\nabla w_j^n\right\|_{C(\tilde{\Omega})} \le \overline{F}(\sigma^n)(\overline{D}_* \overline{G}(\sigma_\pm^*))^n K \le \overline{D}_*^n (\overline{G}(\sigma_\pm^*))^{n+1} K, \tag{3.38}$$

since $\overline{F}(\sigma^n) \le \overline{C}_\epsilon(\sigma^*) \le \overline{G}(\sigma_\pm^*)$ due to the fact $\|\sigma^n - \sigma^*\|_{C^1(\tilde{\Omega})} \le K\theta^n \epsilon < K\epsilon$.

Step 4. Estimate $\left\|\sigma^{n+1} - \sigma^*\right\|_{C^1}$.

From (2.16) we get $\nabla \sigma^{n+1} = 0$ in $\Omega \setminus \tilde{\Omega}$ and then $\sigma^{n+1} = \sigma^*$ in $\Omega \setminus \tilde{\Omega}$. By the same argument as in Step 2, we have

$$\left(I + \epsilon^{n+1} \mathbb{A}[\sigma^*]^{-1} \begin{bmatrix} \frac{\partial w_1^n}{\partial y} & -\frac{\partial w_1^n}{\partial x} \\ \frac{\partial w_2^n}{\partial y} & -\frac{\partial w_2^n}{\partial x} \end{bmatrix}\right) \nabla(\sigma^{n+1} - \sigma^*) = -\epsilon^{n+1} \mathbb{A}[\sigma^*]^{-1} \begin{bmatrix} \frac{\partial w_1^n}{\partial y} & -\frac{\partial w_1^n}{\partial x} \\ \frac{\partial w_2^n}{\partial y} & -\frac{\partial w_2^n}{\partial x} \end{bmatrix} \nabla \sigma^*. \tag{3.39}$$

With the condition (3.26) for ϵ, we have

$$\begin{aligned} \left\|\epsilon^{n+1} \mathbb{A}[\sigma^*]^{-1} \begin{bmatrix} \frac{\partial w_1^n}{\partial y}, & -\frac{\partial w_1^n}{\partial x} \\ \frac{\partial w_2^n}{\partial y}, & -\frac{\partial w_2^n}{\partial x} \end{bmatrix}\right\|_{C(\tilde{\Omega})} &\le \epsilon^{n+1} \left\|\mathbb{A}[\sigma^*]^{-1}\right\|_{C(\tilde{\Omega})} \sqrt{2} \max_{j=1,2} \left\|\nabla w_j^n\right\|_{C(\tilde{\Omega})} \\ &\le \epsilon^{n+1} \left\|\mathbb{A}[\sigma^*]^{-1}\right\|_{C(\Omega)} \sqrt{2} \overline{D}_*^n (\overline{G}(\sigma_\pm^*))^{n+1} K \\ &\le \frac{1}{2} (\epsilon \overline{D}_* \overline{G}(\sigma_\pm^*))^n < \frac{1}{2} \end{aligned} \tag{3.40}$$

due to (3.26), (3.31) and (3.38). So it follows from (3.38), (3.39) and (3.40) that

$$\begin{aligned} \left\|\nabla(\sigma^{n+1} - \sigma^*)\right\|_{C(\tilde{\Omega})} &\le 2\epsilon^{n+1} \left\|\mathbb{A}[\sigma^*]^{-1}\right\|_{C(\tilde{\Omega})} \sqrt{2} \max_{j=1,2} \left\|\nabla w_j^n\right\|_{C(\tilde{\Omega})} \|\nabla \sigma^*\|_{C(\tilde{\Omega})} \\ &\le 2\sqrt{2} K \epsilon^{n+1} \left\|\mathbb{A}[\sigma^*]^{-1}\right\|_{C(\tilde{\Omega})} \overline{D}_*^n (\overline{G}(\sigma_\pm^*))^{n+1} \epsilon. \end{aligned} \tag{3.41}$$

This estimate together with $\left\|\sigma^{n+1} - \sigma^*\right\|_{C^1(\Omega)} \le K \left\|\nabla \sigma^{n+1} - \nabla \sigma^*\right\|_{C(\Omega)}$ generate

$$\left\|\sigma^{n+1} - \sigma^*\right\|_{C^1(\tilde{\Omega})} \le K2 \left\|\mathbb{A}^{-1}[\sigma^*]\right\|_{C(\tilde{\Omega})} \sqrt{2} \overline{D}_*^n (\overline{G}(\sigma_\pm^*))^{n+1} \epsilon^{n+1} K\epsilon \le (\overline{D}_* \overline{G}(\sigma_\pm^*)\epsilon)^{n+1} K\epsilon$$

from (3.25) and (3.29). Now under (3.31) for ϵ, the above estimate leads to

$$\left\|\sigma^{n+1} - \sigma^*\right\|_{C^1(\tilde{\Omega})} \le \theta^{n+1} K\epsilon. \tag{3.42}$$

It is obvious that $\sigma^{n+1} = \sigma^*$ in $\Omega \setminus \tilde{\Omega}$. So (3.34) is also true for $k = n + 1$. The proof is complete. □

3.2 Convergence for three-dimensional medium

Now we consider the convergence in the three-dimensional case. The essence of the proof is almost the same as that in the two-dimensional case, but we need some modifications due to the fact that the harmonic B_z algorithm computes a conductivity distribution in each two-dimensional slice of the three-dimensional medium. More explanations are given in Remark 3.6.

Theorem 3.5. *Assume the target conductivity $\sigma^* \in C^1(\overline{\Omega})$ with $\Omega \subset \mathbb{R}^3$ which satisfies the following conditions:*

A1. $0 < \sigma_-^* \le \sigma^* \le \sigma_+^*$ with known constants $\sigma_\pm^*$;

A2. There exists $\tilde{\Omega} \subset\subset \Omega$ such that σ^* is a known constant in $\Omega \setminus \tilde{\Omega}$;

A3. $|det\ \mathbb{A}[\sigma^*](x,y,z)| \ge d_-^* > 0$ in Ω, where d_-^* is a known constant.

Under these hypotheses, there exist constants $\epsilon = \epsilon(\sigma_\pm^*, d_-^*) > 0$ small enough and $\theta = \theta(\epsilon, \sigma_\pm^*, d_-^*) \in (0,1)$ such that if we take the initial guess σ^0 as the constant $\sigma^*|_{\Omega\setminus\tilde{\Omega}}$, then it holds that the sequence $\{\sigma^n := \sigma^n(x,y,z_0)$ for all $z_0\}$ defined in Ω, where $\sigma^n(x,y,z_0)$ is constructed by the harmonic B_z iteration (2.16) for every z_0, converges to the true conductivity σ^* in Ω for σ^* satisfying

$$\|\nabla\sigma^*\|_{C(\tilde{\Omega})} \le \epsilon. \tag{3.43}$$

More precisely, it holds that

$$\sigma^n = \sigma^* \text{ in } \Omega \setminus \tilde{\Omega}, \tag{3.44}$$

$$\|\sigma^n - \sigma^*\|_{C(\tilde{\Omega})} \le K\theta^n\epsilon, \quad \|\nabla_{x,y}(\sigma^n - \sigma^*)\|_{C(\tilde{\Omega})} \le K\theta^n\epsilon, \quad n = 1, 2, \cdots \tag{3.45}$$

where $K := diam(\Omega) + 1$.

Remark 3.6. In this three-dimensional setting, the estimate (3.45) is given by the $C-$norm while the one in the two-dimensional case in Theorem 3.2 is given by the C^1-norm. We can not improve the derivative estimate $\nabla_{x,y}(\sigma^n - \sigma^*)$ in (3.45) by $\nabla(\sigma^n - \sigma^*)$ since we do not know $\partial_z(\sigma^n - \sigma^*)$, although we have the full three gradient estimates (3.43) for σ^*. The main difficulty in this case is due to the fact that in the iteration process (2.16), we get $\nabla_{x,y}\sigma^{n+1}$ at each slice with no information about $\partial_z\sigma^{n+1}$. That is, the harmonic B_z method approximates the three-dimensional conductivity function $\sigma^*(x,y,z)$ in $\Omega \subset \mathbb{R}^3$ at each two-dimensional slice $\Omega_{z_0} := \Omega \bigcap \{(x,y,z) : z = z_0\} \subset \mathbb{R}^2$. Then σ^n in $\Omega \subset \mathbb{R}^3$, at each iteration, is constructed as $\sigma^n := \bigcup_{z_0} \sigma^n(x,y,z_0)$.

Proof. We also take $\epsilon \in (0, \frac{1}{2K}\sigma_-^*)$. Similarly to the two-dimensional case, we denote by u_j^n and u_j^* the solutions to

$$\begin{cases} \nabla\cdot(\sigma\nabla u_j) = 0, \quad \text{in} \quad \Omega \\ u_j|_{\mathcal{E}_j^+} = 1, \qquad u_j|_{\mathcal{E}_j^-} = 0 \\ -\sigma\nabla u_j \cdot \mathbf{n} = 0 \quad \text{on} \quad \partial\Omega \setminus \mathcal{E}_j^+ \cup \mathcal{E}_j^- \end{cases} \tag{3.46}$$

with $\sigma = \sigma^n$ and σ^*, respectively, and we write σ^0 as $\sigma^0 = \sigma^* + e^0$.

In every slice Ω_{z_0}, we have

$$|e^0(x,y,z_0)| \le diam(\Omega_{z_0}) \left\|\nabla_{x,y}e^0\right\|_{C(\Omega_{z_0})} \le diam(\Omega)\epsilon,$$

hence $\left\|e^0\right\|_{C(\tilde{\Omega})} \le K\epsilon$. Correspondingly, we expand u_j^0 at u_j^* as

$$u_j^0 = u_j^* + \epsilon w_j^0. \tag{3.47}$$

Hence ϵw_j^0 satisfies

$$\begin{cases} \nabla \cdot \left(\sigma^0 \nabla \epsilon w_j^0\right) = -\nabla \cdot (e^0 \nabla u_j^*) \quad \text{in} \quad \Omega \\ \epsilon w_j^0|_{\mathcal{E}_j^+} = 0, \qquad \epsilon w_j^0|_{\mathcal{E}_j^-} = 0 \\ -\sigma^0 \nabla \epsilon w_j^0 \cdot \ \mathbf{n} = (\sigma^0 - \sigma^*) \nabla u_j^* \cdot \ \mathbf{n} = 0 \quad \text{on} \quad \partial\Omega \setminus \mathcal{E}_j^+ \cup \mathcal{E}_j^-. \end{cases} \tag{3.48}$$

In the two-dimensional case, we can estimate the L^2-norm of $(\nabla \cdot e^n \nabla u_j^*)$ by (3.16). This is due to the fact that we can estimate $\|\nabla e^n\|_{C(\Omega)}$. But in the three-dimensional case, it is impossible to estimate $\|\partial_z e^n\|_{C(\Omega)}$. To overcome this difficulty, instead of using the L^2 and the Holder estimates of elliptic problems, we use the L^p estimate with $p > 1$.

First, by applying Lemma 3.1 to (3.46) with $\sigma = \sigma^*$ and the Sobolev imbedding theorem, we deduce that

$$\left\|u_j^*\right\|_{H^2(\tilde{\tilde{\Omega}})} + \left\|\nabla u_j^*\right\|_{C(\tilde{\Omega})} \leq C_* = C_*(\sigma_\pm^*), \tag{3.49}$$

due to (3.43) for $\epsilon \in (0, \frac{1}{2K}\sigma_-^*)$, where $\tilde{\Omega} \subset \tilde{\tilde{\Omega}} \subset \Omega$ and C_* in this three-dimensional case is constructed in the same way as constant $\overline{C}_*$ in (3.13), which implies that the right-hand side of the equation in (3.48) satisfies

$$\|e^0 \nabla u_j^*\|_{L^p(\Omega)} \leq C_* \left\|e^0\right\|_{C(\tilde{\Omega})}, \quad \forall p > 1 \tag{3.50}$$

due to $\sigma^0 = \sigma^1$ on $\Omega \setminus \tilde{\Omega}$. The L^p interior estimates of the problem (3.48) give

$$\|\nabla \epsilon w_j^0\|_{L^p(\tilde{\tilde{\Omega}})} \leq C_4(\sigma^0)[\|\epsilon w_j^0\|_{L^p(\Omega)} + \|e^0 \nabla u_j^*\|_{L^p(\Omega)}]. \tag{3.51}$$

Again by the Sobolev imbedding theorem, $H^1(\Omega) \subset L^p(\Omega)$ with $1 < p \leq 6$, we have

$$\|\epsilon w_j^0\|_{L^p(\Omega)} \leq C_s \|\epsilon w_j^0\|_{H^1(\Omega)} \leq C_s C_1(\sigma^0) \|e^0 \nabla u_j^*\|_{L^2(\Omega)} \leq C_s C_1(\sigma^0) C_* \left\|e^0\right\|_{C(\tilde{\Omega})}.$$

Hence combining this last estimate with (3.49) and (3.51) gives

$$\|\nabla \epsilon w_j^0\|_{L^p(\tilde{\tilde{\Omega}})} \leq C_4(\sigma^0)[C_s C_4(\sigma^0) C_* + C_*] \left\|e^0\right\|_{C(\tilde{\Omega})}. \tag{3.52}$$

Using the difference quotient method of Niremberg with respect to x in (3.48) in $\tilde{\tilde{\Omega}}$ yields

$$\nabla \cdot \sigma^0 \nabla \epsilon D_{x,h} w_j^0 = -\nabla \cdot e^0 \nabla D_{x,h} u_j^* - \nabla \cdot D_{x,h} e^0 \nabla u_{j,x,h}^* - \nabla \cdot D_{x,h} \sigma^0 \nabla \epsilon w_{j,x,h}^0, \tag{3.53}$$

where $D_{x,h} u := \frac{u(x+h,y,z) - u(x,y,z)}{h}$, $u_{x,h}(x,y,z) := u(x+h,y,z)$ with $h < dist(\partial\Omega, \tilde{\tilde{\Omega}})$.

The term in the right-hand side of (3.53) satisfies

$$\begin{cases} \|e^0 \nabla D_{x,h} u_j^*\|_{L^p(\tilde{\tilde{\Omega}})} \leq (1+\epsilon) C_4(\sigma^*) C_* \left\|e^0\right\|_{C(\tilde{\Omega})}, \\ \|D_{x,h} e^0 \nabla u_{j,x,h}^*\|_{L^p(\tilde{\tilde{\Omega}})} \leq C_* \left\|D_{x,h} e^0\right\|_{C(\tilde{\Omega}),} \\ \|D_{x,h} \sigma^0 \nabla \epsilon w_{j,x,h}^0\|_{L^p(\tilde{\tilde{\Omega}})} \leq \left\|D_{x,h} \sigma^0\right\|_{C(\tilde{\tilde{\Omega}})} \|\nabla \epsilon w_j^0\|_{L^p(\tilde{\tilde{\Omega}})}. \end{cases} \tag{3.54}$$

Indeed, $D_{x,h} u_j^*$ satisfies $\nabla \cdot \sigma^* \nabla (D_{x,h} u_j^*) = -\nabla \cdot (D_{x,h} \sigma^*) \nabla u_{j,x,h}^*$ in $\tilde{\tilde{\Omega}}$ from (3.46). Applying the point 4 of Lemma 3.1, we deduce

$$\|\nabla (D_{x,h} u_j^*)\|_{L^p(\tilde{\Omega})} \leq C_4(\sigma^*)[\|D_{x,h} u_j^*\|_{L^p(\tilde{\tilde{\Omega}})} + \|(D_{x,h} \sigma^*) u_{j,x,h}^*\|_{L^p(\tilde{\tilde{\Omega}})}].$$

The estimate $\|D_{x,h} u_j^*\|_{L^p(\tilde{\tilde{\Omega}})} \leq \|\nabla u_j^*\|_{L^p(\tilde{\tilde{\Omega}})}$ and (3.50) give

$$\|\nabla (D_{x,h} u_j^*)\|_{L^p(\tilde{\Omega})} \leq (1+\epsilon) C_4(\sigma^*) C_*,$$

which is the first estimate in (3.54). The second term in (3.54) comes from (3.49).

Again from the interior L^p estimates applied for (3.53), we deduce that $D_{x,h}w_j^0$ is in $W^{1,p}_{loc}(\tilde{\Omega})$ and

$$\begin{aligned}\left\|\epsilon D_{x,h}w_j^0\right\|_{W^{1,p}(\tilde{\Omega})} \quad \leq \quad & (1+C_4(\sigma^0))[\left\|\epsilon D_{x,h}w_j^0\right\|_{L^p(\tilde{\tilde{\Omega}})} + \left\|e^0\nabla D_{x,h}u_j^*\right\|_{L^p(\tilde{\tilde{\Omega}})} + \\ & \left\|D_{x,h}e^0\nabla u^*_{j,x,h}\right\|_{L^p(\tilde{\tilde{\Omega}})} + \|D_{x,h}\sigma^0\nabla\epsilon w^0_{j,x,h}\|_{L^p(\tilde{\tilde{\Omega}})}].\end{aligned} \tag{3.55}$$

Notice that $\left\|\epsilon D_{x,h}w_j^0\right\|_{L^p(\tilde{\tilde{\Omega}})} \leq \left\|\nabla\epsilon w_j^0\right\|_{L^p(\tilde{\tilde{\Omega}})}$ and

$$\left\|D_{x,h}\sigma^0\right\|_{C(\tilde{\tilde{\Omega}})} \leq \left\|\partial_x\sigma^0\right\|_{C(\tilde{\tilde{\Omega}})} \leq \left\|\nabla_{x,y}\sigma^0\right\|_{C(\tilde{\Omega})}. \tag{3.56}$$

The estimate (3.56) is trivial for σ^0 since it is a constant. However, we need this kind of estimate for the iterated sequence $\{\sigma^n\}$ with $\nabla_{x,y}\sigma^n$ continuous in $\tilde{\tilde{\Omega}}$. Hence the estimate (3.55) generates from (3.52), (3.54) and (3.56) that

$$\|\epsilon D_{x,h}w_j^0\|_{W^{1,p}(\tilde{\Omega})} \leq G(\sigma^0)[\left\|e^0\right\|_{C(\tilde{\Omega})} + \left\|D_{x,h}e^0\right\|_{C(\tilde{\Omega})}]$$

for $\epsilon \in (0, \frac{1}{2K}\sigma_-^*)$, where

$$\begin{aligned}&G(\sigma) := (1+C_4(\sigma))C_* \times \\ &\max\left\{[1+\|\nabla_{x,y}\sigma\|_{C(\tilde{\Omega})}]C_4(\sigma)[C_sC_4(\sigma)+1] + (1+\frac{\sigma_-^*}{2K})\sup_{[\sigma_-^*,\sigma_+^*]\times[\frac{1}{\sigma_+^*},\frac{1}{\sigma_-^*}]}F_4(t_1,t_3), 1\right\}.\end{aligned} \tag{3.57}$$

Using the similar estimate, we know that $D_{y,h}w_j^0 \in W^{1,p}_{loc}(\tilde{\Omega})$ and has also the estimate

$$\|\epsilon D_{y,h}w_j^0\|_{W^{1,p}(\tilde{\Omega})} \leq G(\sigma^0)[\left\|e^0\right\|_{C(\tilde{\Omega})} + \left\|D_{y,h}e^0\right\|_{C(\tilde{\Omega})}].$$

Taking the limit with respect to $h \to 0$, we deduce that $\partial_x w_j^0,\ \partial_y w_j^0 \in W^{1,p}_{loc}(\tilde{\Omega})$ and

$$\|\epsilon\partial_x w_j^0\|_{W^{1,p}(\tilde{\Omega})},\ \ \|\epsilon\partial_y w_j^0\|_{W^{1,p}(\tilde{\Omega})} \leq G(\sigma^0)[\left\|e^0\right\|_{C(\tilde{\Omega})} + \left\|\nabla_{x,y}e^0\right\|_{C(\tilde{\Omega})}]$$

from which the Sobolev imbedding theorem $W^{1,p}(\tilde{\Omega}) \subset C(\tilde{\Omega})$ for $p > 3$ implies

$$\|\epsilon\partial_x w_j^0\|_{C(\tilde{\Omega})},\ \ \|\epsilon\partial_y w_j^0\|_{C(\tilde{\Omega})} \leq C_sG(\sigma^0)[\left\|e^0\right\|_{C(\tilde{\Omega})} + \left\|\nabla_{x,y}e^0\right\|_{C(\tilde{\Omega})}].$$

We set $F(\sigma) := C_sG(\sigma)$ with $G(\sigma)$ defined in (3.57) and the constant $C_\epsilon(\sigma^*) := \sup_{\mathbb{S}_3}F(\sigma)$ with

$$\mathbb{S}_3 := \{\sigma(x,y,z) : \|\sigma-\sigma^*\|_{C(\Omega)} \leq K\epsilon,\ \|\nabla_{x,y}\sigma\|_{C(\tilde{\Omega})} \leq (K+1)\epsilon\}.$$

Again, noticing that $F(\sigma)$ contains only F_1, F_4, the constant $C_\epsilon(\sigma^*)$ can be estimated by

$$C_\epsilon(\sigma^*) \leq \sup_{\mathbb{S}_4}F(\sigma) =: G(\sigma_\pm^*) \tag{3.58}$$

for $\epsilon \in (0, \frac{1}{2K}\sigma_-^*)$, where

$$\mathbb{S}_4 := \left\{\sigma(x,y,z) : \frac{1}{2}\sigma_-^* < \sigma < \frac{1}{2}\sigma_-^* + \sigma_+^*,\ \|\nabla_{x,y}\sigma\|_{C(\tilde{\Omega})} \leq \frac{K+1}{2K}\sigma_-^*\right\}.$$

In particular, we have $C_s G(\sigma^0) \le G(\sigma^*_\pm)$. Then the above estimate reads as

$$\|\epsilon\partial_x w_j^0\|_{C(\tilde\Omega)},\ \|\epsilon\partial_y w_j^0\|_{C(\tilde\Omega)} \le G(\sigma^*_\pm)[\left\|e^0\right\|_{C(\tilde\Omega)} + \left\|\nabla_{x,y} e^0\right\|_{C(\tilde\Omega)}]. \tag{3.59}$$

Obviously, (3.59) is also true in $\tilde\Omega_{z_0} := \tilde\Omega \bigcap \{(x,y,z) : z = z_0\} \subset \mathbb{R}^2$ for any z_0, that is,

$$\|\epsilon\partial_x w_j^0\|_{C(\tilde\Omega_{z_0})},\ \|\epsilon\partial_y w_j^0\|_{C(\tilde\Omega_{z_0})} \le G(\sigma^*_\pm)[\left\|e^0\right\|_{C(\tilde\Omega)} + \left\|\nabla_{x,y} e^0\right\|_{C(\tilde\Omega)}],$$

which corresponds to (3.21) in the two-dimensional case. As for (3.25) in the two-dimensional case, we have

$$\left\|\mathbb{A}[\sigma^*]^{-1}\right\|_{C(\tilde\Omega_{z_0})} \le \left\|\mathbb{A}[\sigma^*]^{-1}\right\|_{C(\tilde\Omega)} \le \frac{\sqrt{2}}{d^*_-} C_* \tag{3.60}$$

for any z_0 due to A2. We choose $\epsilon \in (0, \frac{1}{2K}\sigma^*_-)$ small enough such that

$$\epsilon \left\|\mathbb{A}[\sigma^*]^{-1}\right\|_{C(\tilde\Omega)} \sqrt{2} G(\sigma^*_\pm) K \le \frac{2\epsilon C_* G(\sigma^*_\pm) K}{d^*_-} < \frac{1}{2}, \tag{3.61}$$

then we get from the same argument as that in subsection 3.1 that

$$\begin{aligned} \|\nabla_{x,y}(\sigma^* - \sigma^1)\|_{C(\tilde\Omega_{z_0})} &\le 2\|\mathbb{A}[\sigma^*]^{-1}\|_{C(\tilde\Omega_{z_0})}\sqrt{2}\|\epsilon\nabla_{x,y} w_j\|_{C(\tilde\Omega_{z_0})}\|\nabla_{x,y}\sigma^*\|_{C(\tilde\Omega_{z_0})} \\ &\le 2\sqrt{2}\|\mathbb{A}[\sigma^*]^{-1}\|_{C(\tilde\Omega)} G(\sigma^*_\pm) K\epsilon^2. \end{aligned} \tag{3.62}$$

As for $\sigma^1 - \sigma^*$, we have the estimate $\left\|\sigma^1 - \sigma^*\right\|_{C(\tilde\Omega_{z_0})} \le K \left\|\nabla_{x,y}(\sigma^1 - \sigma^*)\right\|_{C(\tilde\Omega_{z_0})}$, hence

$$\left\|\sigma^1 - \sigma^*\right\|_{C(\tilde\Omega)} \le K 2\sqrt{2} \left\|\mathbb{A}[\sigma^*]^{-1}\right\|_{C(\tilde\Omega)} G(\sigma^*_\pm) K\epsilon^2. \tag{3.63}$$

For each $\sigma^1(x,y,z_0)$ generated by the harmonic B_z method at each slice $\tilde\Omega_{z_0}$, we generate σ^1 in $\tilde\Omega \subset \mathbb{R}^3$ by $\sigma^1 := \bigcup_{z_0} \sigma^1(x,y,z_0)$. Now for $\epsilon \in (0, \frac{1}{2K}\sigma^*_-)$ satisfying (3.61),

$$K2\sqrt{2}\|\mathbb{A}[\sigma^*]^{-1}\|_{C(\tilde\Omega)} G(\sigma^*_\pm)\epsilon \le \frac{4}{d^*_-} C_* K G(\sigma^*_\pm)\epsilon := D_* G(\sigma^*_\pm)\epsilon := \theta \in (0,1), \tag{3.64}$$

then it follows that

$$\|\nabla_{x,y}(\sigma^1 - \sigma^*)\|_{C(\tilde\Omega)},\ \left\|\sigma^1 - \sigma^*\right\|_{C(\tilde\Omega)} \le K\theta\epsilon,$$

which means $F(\sigma^1) \le C_\epsilon(\sigma^*) \le G(\sigma^*_\pm)$. As in the two-dimensional case, we have $\sigma^1 = \sigma^*$ in $\Omega \setminus \tilde\Omega$. So the theorem is true for $n = 1$. It follows from (3.61) and (3.64) that $\epsilon = \epsilon(\sigma^*_\pm, d^*_-), \theta = \theta(\epsilon, \sigma^*_\pm, d^*_-)$.

Now, we can apply the induction argument to prove the theorem. That is, assume that $\sigma^k \equiv \sigma^*$ in $\Omega \setminus \tilde\Omega$ and the following estimates

$$\|\nabla_{x,y}(\sigma^k - \sigma^*)\|_{C(\tilde\Omega)},\ \left\|\sigma^k - \sigma^*\right\|_{C(\tilde\Omega)} \le K(D_* G(\sigma^*_\pm)\epsilon)^k \epsilon = K\theta^k\epsilon$$

are true for $k = n$. We shall prove that this is also true for $k = n+1$.

This can be done by the same way as in the two-dimensional case, with the same modifications for the three-dimensional case as those given for the proof of this theorem in the step $n = 1$. Indeed, $\nabla_{x,y}\sigma^n$ is continuous in every slice Ω_{z_0} from its definition (2.16) for $\sigma^* \in C^1$. This fact implies that (3.56) is true with σ^0 replaced by σ^n. Moreover, we have $C_s G(\sigma^n) \le C_\epsilon(\sigma^*) \le G(\sigma^*_\pm)$ from the assumption of the induction argument. So we omit the details. □

4 Numerical performance

We present some numerics to show our theoretical convergence property. For simplicity, we deal with the axially symmetric case where input current densities in the electrodes are specified. That is, the governed system is the following two-dimensional problem for potential $u = u(x, y)$:

$$\begin{cases} \nabla \cdot (\sigma \nabla u) = 0 & \text{in } \Omega \\ -\sigma \nabla u \cdot \mathbf{n} = g(x, y) & \text{on } \partial\Omega \end{cases} \tag{4.1}$$

with $u(0, 0) = 0$ at the reference point $(0, 0)$. Consider the target conductivity in $\Omega := [-1, 1] \times [-2, 2]$ of the form

$$\sigma^*(r) = \begin{cases} 3 & \text{if} \quad 0 \le r \le 0.4 \\ -10r^2 + 4.6 & \text{if} \quad 0.4 \le r \le 0.6, \\ 1 & \text{otherwise,} \end{cases} \tag{4.2}$$

where $r = \sqrt{x^2 + y^2}$. Electrodes are specified as $\mathcal{E}_1^{\pm} := \{(\pm 1, y) : |y| < 0.1\}$ and $\mathcal{E}_2^{\pm} := \{(x, \pm 2) : |x| < 0.1\}$ on $\partial\Omega$. The input current densities $g^j, j = 1, 2$ are given by

$$g^j|_{\mathcal{E}_j^{\pm}} = \pm 1 \quad \text{and} \quad g^j = 0 \quad \text{on } \partial\Omega \setminus [\mathcal{E}_j^+ \cup \mathcal{E}_j^-]. \tag{4.3}$$

The corresponding $\nabla^2 B_z^j = \mu_0(\sigma_x u_y^{j,*} - \sigma_y u_x^{j,*})$ are shown in Figure 4, where $u^{j,*}$ is the solution corresponding to (σ^*, g_j) for $j = 1, 2$.

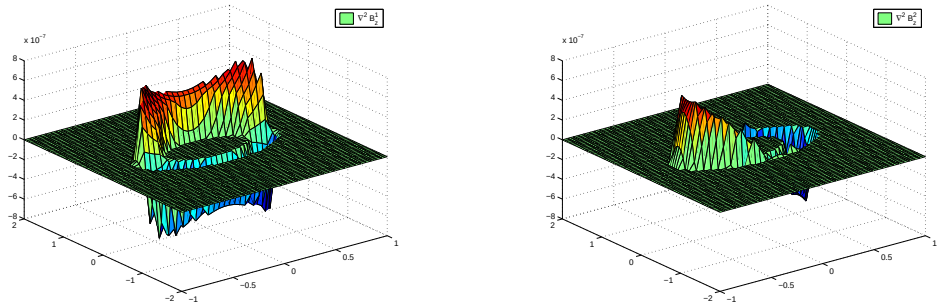

Figure 4: Distributions of $\nabla^2 B_z^1$, $\nabla^2 B_z^2$

We introduce $\Phi(\mathbf{r}, \mathbf{r}') = \frac{1}{2\pi} \ln |\mathbf{r} - \mathbf{r}'|$ and divide Ω into $N \times M$ small rectangles. Denote by $\mathbf{r}_{k,l}$ the center of each rectangle $e(k, l)$. Then a simple computation generates the following discrete iteration formula:

$$\sigma^{n+1}(\mathbf{r}_{k,l}) = f(\mathbf{r}_{k,l}) - \frac{1}{\mu_0} \sum_{i,j=1}^{N,M} \int_{e(i,j)} \nabla\Phi(\mathbf{r}', \mathbf{r}_{k,l}) \cdot \mathbb{A}[\sigma^n]^{-1} \begin{pmatrix} \nabla^2 B_z^1 \\ \nabla^2 B_z^2 \end{pmatrix} (\mathbf{r}') d\mathbf{r}', \tag{4.4}$$

where $f(\mathbf{r}) = \int_{\partial\Omega} \nabla_{\mathbf{r}'} \Phi(\mathbf{r}, \mathbf{r}') \cdot \mathbf{n}_{\mathbf{r}'} \, \sigma^*(\mathbf{r}') ds(\mathbf{r}')$.

For the integrals in the elements, where we take $\mathbb{A}[\sigma^n]^{-1}, \nabla^2 B_z$ as constants at each elements, they are zero for $(i, j) = (k, l)$ due to the symmetric property (noticing that $\mathbf{r}_{k,l}$ is the center of $e(k, l)$), and regular for $(i, j) \neq (k, l)$. So we can construct the sequence $\{\sigma^n\}$ inside Ω for a given initial guess $\sigma^0(\mathbf{r})$.

In our numerical test, the finite element method with bilinear base functions $\phi^{i,j}(x,y) = (a+by)(c+dy)$ at each nodal point are used to solve the direct problem for $u[\sigma^n]$ at each iteration step. Then $\nabla u[\sigma^n]$ at the center of each element can be computed by the difference method. We also use this scheme to simulate $\nabla^2 B_z$ from (4.1)-(4.3) for our inversion input. To avoid the well-known *inverse crime* in the numerical tests [7], we use different grids in simulating the input data from those used in the inversion algorithm.

First, we take $N = 40, M = 80$ (case 1) and the initial guess function $\sigma_0(x,y) \equiv 1$. The recovering result after six iterations, as well as the exact one are shown in Figure 5. Now we choose a finer mesh with $N = 80, M = 160$ (case 2). Denote by $E(n)$ the relative L^2- error between the target conductivity and the reconstructed one after nth iteration. The numerical values of $E(n)$ in these two cases are given in Table 1 while curves are plotted in Figure 6 for a bigger iteration number $n = 10$.

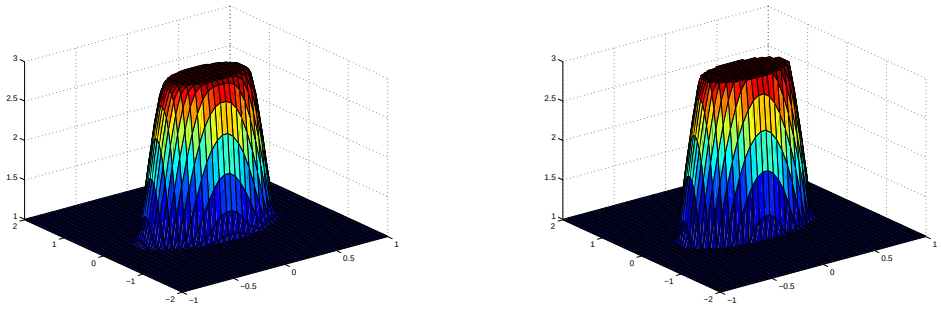

Figure 5: Reconstruction after six iterations (left) and the exact one (right).

Table 1 Relative L^2 error $E(n)$ in two cases.

n	case 1	case 2	n	case 1	case 2
0	0.449118	0.449185	4	0.035278	0.028515
1	0.226044	0.224892	5	0.024009	0.015632
2	0.114281	0.111283	6	0.019200	0.009711
3	0.060467	0.055545	7	0.017172	0.007149

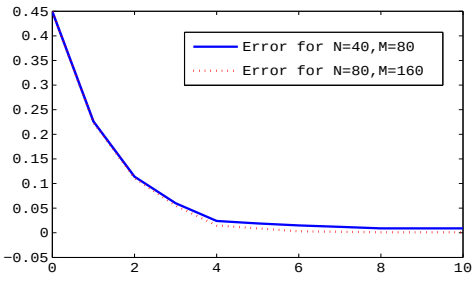

Figure 6: $E(n)$ with respect to the iteration number n for two different meshes.

From the error distributions in Figure 6 and Table 1, we can observe that the iteration algorithm converges very quickly. In fact, the error is almost unchanged after six iterations.

This phenomena matches very well with our theoretical result which assumes a convergence rate of the order θ^n with $\theta \in (0,1)$. The excellent convergence performance comes from our good initial guess $\sigma^0 \equiv 1$. This means that the error of ϵ for the initial guess is not so large and θ will be also small for small ϵ. We can also observe that the finer mesh can improve the inversion result at the expense of an increased amount of computations.

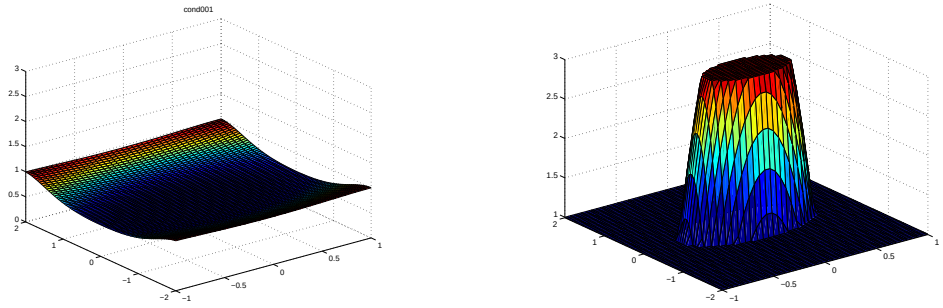

Figure 7: Inferior initial guess σ^0 (left) and the exact σ^* (right).

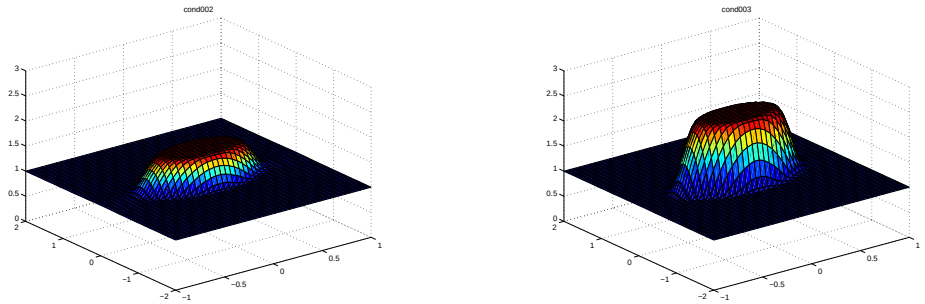

Figure 8: Reconstruction for $n = 1$ (left) and $n = 2$ (right) using the inferior initial guess.

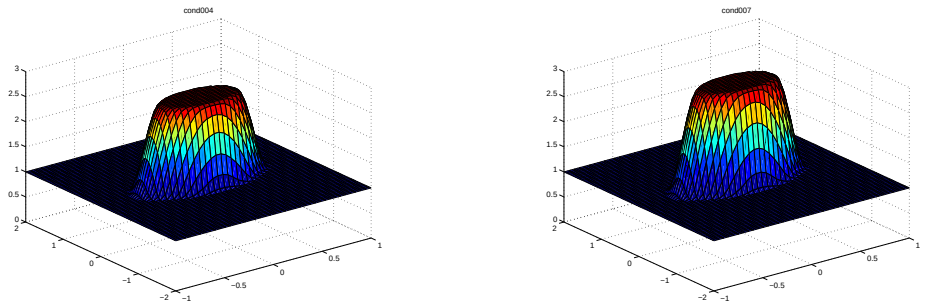

Figure 9: Reconstruction for $n = 3$ (left) and $n = 6$ (right) using the inferior initial guess.

Now let us consider an inferior initial guess function

$$\sigma^0(x,y) = \frac{4}{5} - \frac{1}{5}\cos\frac{(x^2+y^2)\pi}{5}, \tag{4.5}$$

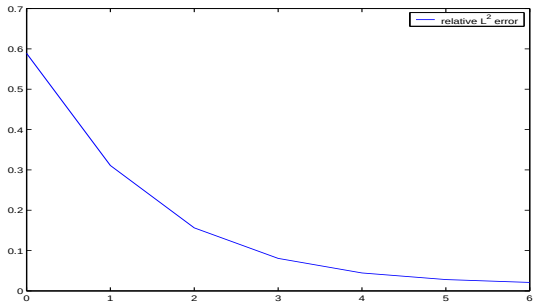

Figure 10: Relative error distribution for the inferior initial guess.

which is quite different from the exact $\sigma^*(x, y)$, see Figure 7. The reconstruction results for $n = 1, 2, 3, 6$ are given in Figure 8 and 9 with its error distribution illustrated in Figure 10. Even for this case with the undesirable initial guess, we can see that the algorithm still catches the target σ^* in the whole domain.

It should be noticed that we used the simulation data $\nabla^2 B_z^j, j = 1, 2$ directly for the harmonic B_z algorithm, rather than computing $\nabla^2 B_z^j$ from B_z^j. Obviously, if we use noisy measured B_z data as the inversion input, a suitable denoiseing technique must be used. Noticing the expression of the iteration (2.16), the harmonic B_z algorithm uses in fact the first derivative of B_z. A similar inversion scheme using the first derivative of B_z named the gradient B_z method can be found in [18, 19].

Acknowledgements: This work was supported by the SRC/ERC program of MOST/ KOSEF (R11-2002-103 and R01-2005-000-10339-0). The first author was also supported by NSFC (No.10371018) and Impedance Imaging Research Center (IIRC) at Kyung Hee University. The third author was supported by BK21 project at Yonsei University and IIRC at Kyung Hee University. We would like to thank a referee for pointing out new references about the condition (2.11) in the Remark 2.5.

References

[1] G. Alessandrini, E. Rosset and J. K. Seo, *Optimal size estimates for the inverse conductivity poblem with one measurement*, Proc. Amer. Math. Soc., 128(2000), pp.53-64.

[2] G. Alessandrini and R. Magnanini, *The index of isolated critical points and solutions of elliptic equations in the plane*, Ann. Scoula. Norm. Sup. Pisa Cl Sci., 19(1992), pp.567-589.

[3] G.Alessandrini, V.Nesi, *Univalent σ-harmonic mappings*, Arch. Rational Mech. Anal., 50 (2001), no. 2, pp.747-757.

[4] P. Bauman, A. Marini, V. Nesi, *Univalent solutions of an elliptic system of partial differential equations arising in homogenization*, Indiana Univ. Math. J., 128(2000), pp.53-64.

[5] M. Briane, G.W. Milton, V. Nesi, *Change of sign of the correctors determinant for homogenization in three-dimensional conductivity*, Arch. Ration. Mech. nal, 173 (2004), no.1, pp.133-150.

[6] M. Cheney, D. Isaacson and J. C. Newell, *Electrical impedance tomography*, SIAM Review, 41(1999), pp.85-101.

[7] D. Colton and R. Kress, *Inverse Acoustic and Electromagnetic Scattering Theory*, 2nd edition, Springer-Verlag, Berlin, (1998).

[8] G. Difazio, *L^p estimates for divergence form elliptic equations with discontinuous coefficients*, Boll. Un. Mat. Ital. A, 10(1996), pp.409-420.

[9] G. B. Folland, *Introduction to Partial Differential Equations*, Princeton University Press, Princeton, New Jersey, 1976.

[10] D. Gilbarg and N. S. Trudinger, *Elliptic Partial Differential Equations of Second Order*, Springer-Verlag, 2001.

[11] Y. Z. Ider, S. Onart and W. Lionheart, *Uniqueness and reconstruction in magnetic resonance-electrical impedance tomography (MR-EIT)*, Physiol. Meas., 24(2003), pp.591-604.

[12] O. Kwon, C. Park, E. J. Park, J. K. Seo and E. J. Woo, *Electrical conductivity imaging using a variational method in B_z-based MREIT*, Inverse Problems, 21(2005), pp.969-980.

[13] R.S. Laugesen, *Injectivity can fail for higher-dimensional harmonic extensions*, Complex Variables, 28 (1996), pp. 357-369.

[14] J. J. Liu, H. C. Pyo, J. K. Seo and E. J. Woo, *Convergence properties and stability issues in MREIT algorithm*, to appear in Contemporary Mathematics.

[15] S. Lee, J. K. Seo, C. J. Park, B. I. Lee, E. J. Woo, S. Y. Lee, O. Kwon and J.Hahn, *Conductivity image reconstruction from defective data in MREIT: numerical simulation and animal experiment*, IEEE Trans. Med. Imag., 25(2006), pp.168-176.

[16] P. Metherall, D. C. Barber, R. H. Smallwood and B. H. Brown, *Three-dimensional electrical impedance tomography*, Nature, 380(1996), pp.509-512.

[17] S. H. Oh, B. I. Lee, E. J. Woo, S. Y. Lee, T. S. Kim, O. Kwon and J. K. Seo, *Electrical conductivity images of biological tissue phantoms in MREIT*, Physiol. Meas., 26(2005), pp.279-288.

[18] C. Park, E. J. Park, E. J. Woo, O. Kwon and J. K. Seo, *Static conductivity imaging using variational gradient B_z algorithm in magnetic resonance electrical impedance tomography*, Physiol.Meas., 25(2004), pp.257-269.

[19] C. Park, O. Kwon, E. J. Woo and J. K. Seo, *Electrical conductivity imaging using gradient B_z decomposition algorithm in magnetic resonance electrical impedance tomography (MREIT)*, IEEE Trans. Med. Imag., 23(2004), pp.388-394.

[20] J. K. Seo, J. R. Yoon, E. J. Woo and O. Kwon, *Reconstruction of conductivity and current density images using only one component of magnetic field measurements*, IEEE Trans. Biomed. Eng., 50(2003), pp.1121-1124.

[21] J. K. Seo, O. Kwon, B. I. Lee and E. J. Woo, *Reconstruction of current density distributions in axially symmetric cylindrical sections using one component of magnetic flux density: computer simulation study*, Physiol. Meas., 24(2003), pp.565-577.

[22] J. K. Seo, *On the uniqueness in the inverse conductivity problem*, J. Fourier Anal. Appl., 2(1996), pp.227-235.

[23] J. K. Seo, H. C. Pyo, C. Park, O. Kwon, and E. J. Woo, *Image reconstruction of anisotropic conductivity tensor distribution in MREIT: computer simulation study*, Phys. Med. Biol., 49(2004), pp.4371-4382.

[24] G. Verchota, *Layer potentials and boundary value problems for Laplace's equation in Lipschitz domains*, J. of Func. Anal., 59(1984), pp.572-611.

[25] J. G. Webster, *Electrical Impedance Tomography*, Adam Hilger, Bristol, UK, 1990.